frontiers | Frontiers in Earth Science

TYPE Original Research
PUBLISHED 04 December 2024
DOI 10.3389/feart.2024.1507359



OPEN ACCESS

EDITED BY
Junwen Peng,
University of Oklahoma, United States

REVIEWED BY
Ling Guo,
Northwest University, China
Haibo Jia,
Shandong University of Science and Technology, China

*CORRESPONDENCE
Jie Xu,
jiexu@cugb.edu.cn

RECEIVED 07 October 2024
ACCEPTED 20 November 2024
PUBLISHED 04 December 2024

CITATION
Wen J, Xu J, Jiang Z, Liu T, Meng J, Zhang J, Wei S, Shen Z, Li Y and Zhang X (2024) A volcanic and gravity flow controlled fine-grained organic rich deposits of the lower Jurassic Beipiao formation in the Western Liaoning, northeast China. *Front. Earth Sci.* 12:1507359. doi: 10.3389/feart.2024.1507359



# A volcanic and gravity flow controlled fine-grained organic rich deposits of the lower Jurassic Beipiao formation in the Western Liaoning, northeast China

Jiucun Wen[1,2,3], Jie Xu[1,2,3]*, Zaixing Jiang[4], Tong Liu[4], Jiayi Meng[4], Jiazhi Zhang[4], Siyuan Wei[4], Zhihan Shen[4], Yongfei Li[5,6] and Xi Zhang[7]

[1]School of Ocean Sciences, China University of Geosciences (Beijing), Beijing, China, [2]Key Laboratory of Polar Geology and Marine Mineral Resources, China University of Geosciences (Beijing), Beijing, China, [3]Hainan institute of China University of Geosciences (Beijing), China University of Geosciences (Beijing), Sanya, Hainan, China, [4]School of Energy Resources, China University of Geosciences (Beijing), Beijing, China, [5]Shenyang Geological Survey Center, China Geological Survey, Shenyang, China, [6]Observation and Research Station of Mesozoic Stratigraphic System in western Liaoning, China Geological Survey, Shenyang, China, [7]SINOPEC Northeast Oil & Gas Branch, Exploration and Development Research Institute, Changchun, China

**Introduction:** The Lower Jurassic Beipiao Formation in the western Liaoning of northeast China represents a significant case study for understanding the interplay between volcanic activity, sedimentary processes, and organic matter enrichment.

**Methods:** This study aims to investigate the lithofacies, depositional environments, and hydrocarbon potential of the Beipiao Formation, using core, outcrop, thin-section, and geochemical data.

**Results:** Thirteen lithofacies types were identified, which reflect a complex depositional history influenced by volcanic processes and gravity flows. The sedimentary facies analysis revealed three key depositional environments: shallow lake, semi-deep to deep lacustrine, and fan delta. The basin evolution suggests a transition from fan delta deposits to deep lake deposits and then back to fan delta, with volcanic and gravity flow deposits interbedded. Volcanic activity not only provided nutrient-rich environments conducive to biological productivity but also helped create conditions favorable for organic matter preservation. The earthquake, flooding or stormed events induced gravity flow, which favored plant fragments dispersal to the deep-lake and formed type III kerogen in the deep-lake developed area.

**Discussion:** These findings suggest that the Jurassic Beipiao Formation in western Liaoning Province, exhibit significant hydrocarbon potential. This challenges previous assumptions regarding the dominance of shallow water environments and limited exploration prospects within the Yanshan Orogenic Belt. Furthermore, this study highlights the crucial role of volcanic activity and gravity flow in organic matter enrichment, transportation, and preservation

within a volcanic-rift basin, with potential applicability to similar basins worldwide.

KEYWORDS

**Beipiao formation, gravity flow, volcanic process, black shale, organic matter**

## 1 Introduction

Volcanic eruptions release substantial amounts of material and energy, significantly impacting the atmosphere, hydrosphere, and biosphere. Recently, an increasing number of oil- and gas-bearing black mudstones have been found to originate closely in relation to volcanic activity (Zhou et al., 1989; Wang et al., 2013; Aarnes et al., 2010; Felipe et al., 2007; Aarnes et al., 2015). Numerous studies indicate that since the Cambrian, organic carbon burial and the formation of shale oil and gas in multiple marine basins are often associated with global or regional high-frequency volcanic activities (e.g., Trabucho-Alexandre et al., 2012; Abrajevitch et al., 2014; Lee et al., 2018; Lu et al., 2020). Extensive oil and gas explorations in China have also discovered abundant shale oil and gas resources associated to some extent with volcanic-hydrothermal activities. Examples include the Permian Lucaogou Formation in the Malang Depression of the Santanghu Basin (Wang et al., 2013; Jiao et al., 2021; Fan, 2004), the Upper Triassic Yanchang Formation in the Ordos Basin (Zou et al., 2019; Yuan et al., 2019), the Permian Lucaogou Formation in the Jimusar Depression of the Junggar Basin (Qu et al., 2019a), and the Ordovician–Silurian Wufeng–Longmaxi Formation in the southern Yangtze region (Qiu et al., 2018; Du et al., 2022).

Observations of outcrops and cores in the Chang 7 Member of the Ordos Basin reveal that organic-rich shale layers are interbedded with multiple tuff layers, ranging from millimeters to centimeters in thickness. Statistical analyses show that an increased number of sedimentary tuff layers correlates with greater source rock thickness and higher total organic carbon (TOC) values (Zhang R. et al., 2017). Lu et al. (2022) suggested that volcanic ash induces reducing conditions and promotes the deposition of pyrite layers, which favor the preservation of organic matter in shale. Therefore, strong links exist between volcanic activity and organic matter enrichment in black shale.

In this study, we investigate the Lower Jurassic Beipiao Formation in the Western Liaoning to examine the influence of depositional processes and volcanic activity on organic enrichment in black shale. Despite earlier beliefs that the Mesozoic basins of the Yanshan orogenic belt lacked significant hydrocarbon potential due to predominant shallow-water deposits and severely eroded reservoirs (Wu et al., 2004; Jia et al., 2019a; Dou et al., 2020), recent findings have challenged this perspective. The discovery of shale oil in the Cretaceous Xiguayuan Formation of the Luanping Basin in 2020 (Well Luantan-1) overturned the traditional view that Mesozoic strata in this region are barren of oil, emphasizing the role of volcanic activity in hydrocarbon generation and preservation (Yuan et al., 2020).

Similarly, the western Liaoning, part of the Yanshan tectonic belt, has its Mesozoic tectonic and sedimentary evolution strongly influenced by the Yanshanian movement and related volcanism. Recent hydrocarbon shows in the Lower Jurassic Beipiao Formation within the Beipiao-Jinyang Basin in the western Liaoning suggest significant exploration potential (Chen et al., 2013; Sun S. L. et al., 2019; Li and Chen, 2014; Zhang et al., 2015). Observations indicate that, contrary to previous beliefs of a purely shallow-water coal-bearing environment, the Beipiao Formation also contains deep-water lacustrine deposits, including black mudstones with gravity flow characteristics and volcaniclastic sediments (Zhang et al., 2016). Volcanic activity during the deposition of the Beipiao Formation may have played a crucial role in organic matter enrichment and hydrocarbon accumulation.

Therefore, this study aims to reevaluate the influence of depositional processes and volcanic activity on organic enrichment in the Lower Jurassic Beipiao Formation of the Western Liaoning. By systematically analyzing lithofacies and sedimentary environments based on core samples, outcrop profiles, thin-section and geochemical data, we seek to provide theoretical support for selecting favorable zones and guiding future exploration efforts.

## 2 Geological background

The Western Liaoning, located in the eastern part of the Yanshan orogenic belt, contain several Mesozoic lacustrine basins, including Beipiao Basin, Jinyang Basin, Jianchang-Kazuo Basin and Chaoyang Basin (Figure 1). It is bounded to the northwest by the nearly east-west-trending axial uplift known as the Inner Mongolia Axis, to the south by the Shanghaiguan Platform Arch, and to the east by the Beizhen Uplift, which separates it from the North China Rift (Yan et al., 2003; Wang et al., 2001). Since the end of the Middle Triassic, influenced by the Indosinian and Yanshanian orogenies, the region's folds and faults predominantly trend northeast, forming a structural pattern of alternating basement uplifts—composed of Archean to Paleozoic rocks—and Mesozoic to Cenozoic basins (Figure 1) (Zhen et al., 2016; Lin, 2019; Liu, 2019). Since the Jurassic, the Yanshan Orogeny has been the dominant geological force shaping basin structure, sedimentary filling, and paleontological evolution in northeast China. The Yanshan Orogeny is generally divided into three major stages: a strong compressional stage (175–136 Ma), a primary extensional stage (135–90 Ma), and a weak compression-deformation stage (~80 Ma) (Dong et al., 2018). The Beipiao Formation formed during the first stage of strong regional compression and developed between two significant pulses of volcanic activity, as evidenced by the widespread volcanic rocks of the underlying Xinglonggou Formation and the overlying Tiaojishan Formation (Figure 2). During the Late Jurassic, volcanic eruptions of the Yixian Formation induced strong compressional torsion within the basin, leading to the formation of the Nantianmen Fault Zone. This fault zone exposed Middle to Late Proterozoic and Paleozoic carbonates, as well as Mesozoic volcanic rocks, effectively

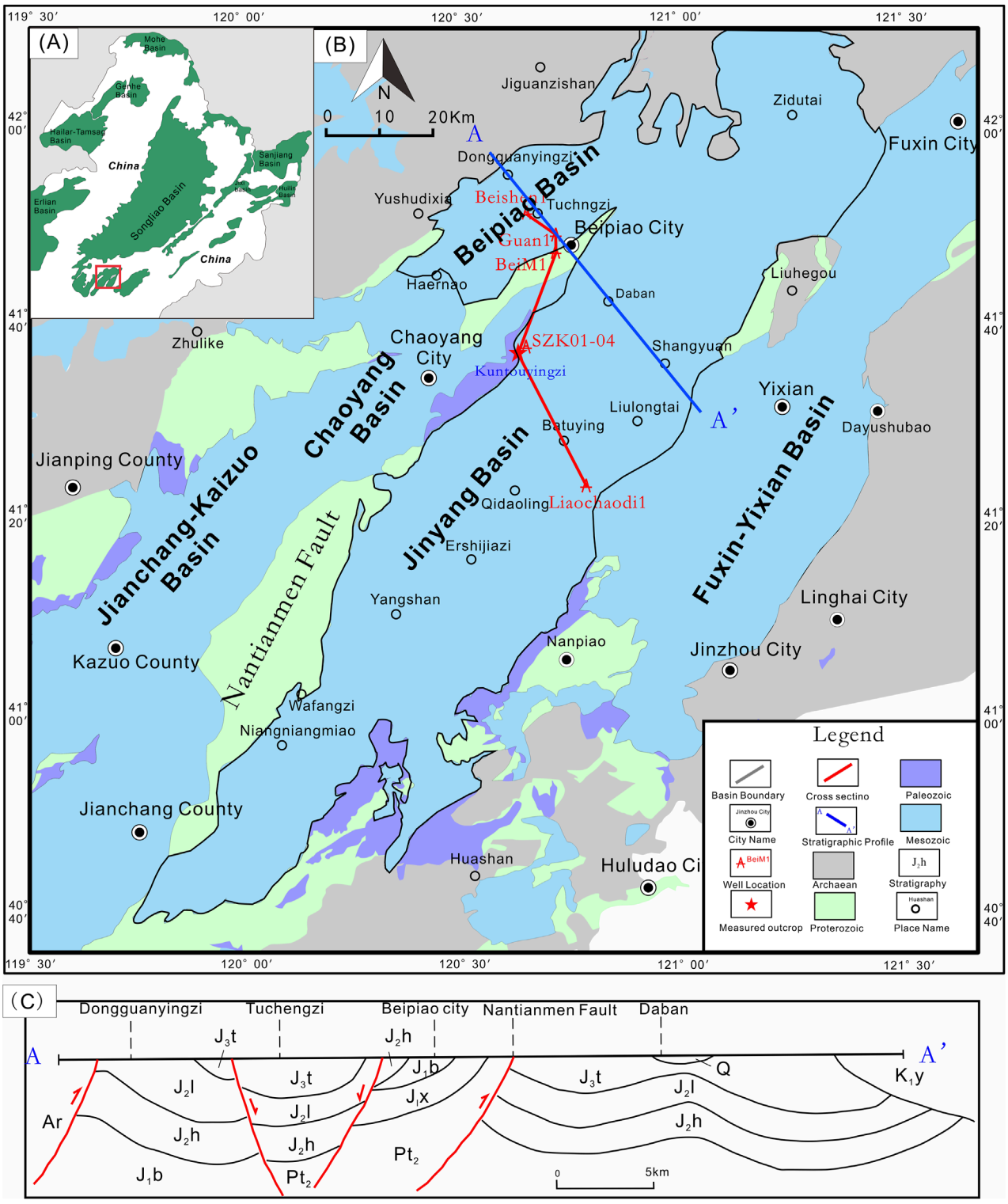


FIGURE 1
Overview of the study area. **(A)** The Mesozoic basin distribution in the Western Liaoning (modified after Deng et al., 2022); **(B)** Cross section A-A1(From Yang et al., 2003); **(C)** A-A' Stratigraphic profile.

dividing the large basin present during the deposition of the Lower Jurassic Beipiao Formation into the current Beipiao and Jinyang basins (Yan et al., 2003; Wang et al., 2001; Zhou and Zhao, 1999).

Prior to the Late Triassic, the region underwent basin basement evolution. The basin variably exposes Archean Jianping and Fuping groups; Mesoproterozoic and Neoproterozoic Changcheng, Jixian,

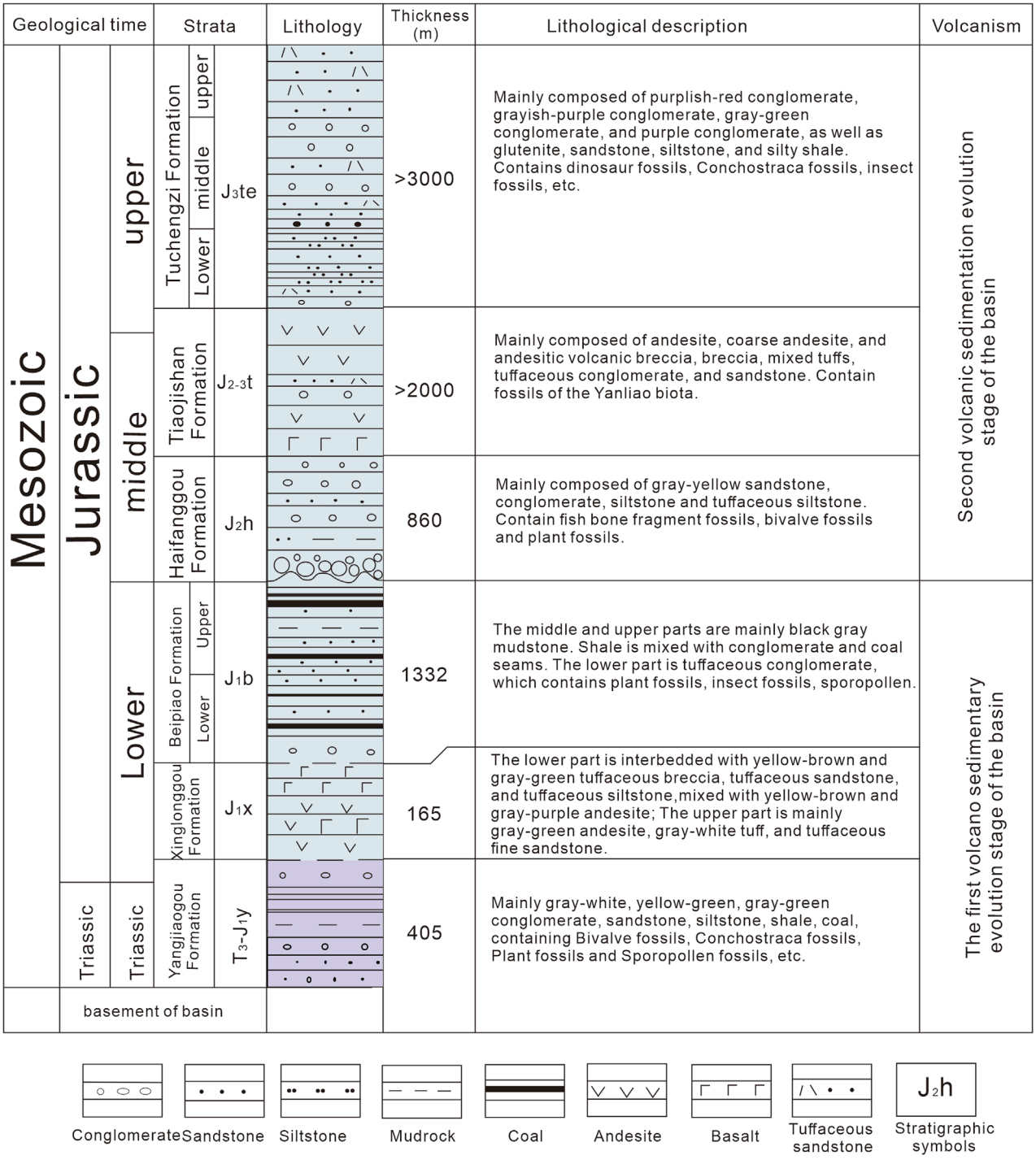


FIGURE 2
Comprehensive stratigraphic column of the mesozoic in the western liaoning (modified after Yan et al., 2002; Yan et al., 2003).

and Qingbaikou systems; and Paleozoic Cambrian, Ordovician, Carboniferous, Permian, and Lower to Middle Triassic strata. Since the end of the Middle Triassic, the area experienced intense tectono-magmatic reactivation under an overall compressive stress regime, undergoing two complete volcanic-sedimentary cycles. This led to the development of a northeast to north–northeast-trending structural pattern of alternating basins and ranges. Extensive Mesozoic volcanic-sedimentary sequences were deposited within the basin, with the Jurassic strata being particularly well developed. From bottom to top, these include the Xinglonggou Formation, Beipiao Formation, Haifanggou Formation, Lanqi Formation, and Tuchengzi Formation (Figure 2) (Yan et al., 2002; 2003).

The focus of this study is the Jurassic Beipiao Formation. Following the volcanic eruptions of the Xinglonggou Formation,

the Beipiao-Jinyang Basin underwent differential subsidence and further expansion, experiencing a significant lacustrine transgression. This event led to the deposition of lacustrine sediments characterized mainly by lake systems accompanied by volcanic sedimentary features (Zhen et al., 2016).

Previous studies have considered the Beipiao Formation in western Liaoning as a set of coal-bearing strata, suggesting an overall shallow-water environment (He et al., 2006; Wang, 2011). However, some researchers have observed gray-black sandstone, mudstone, and shale in core samples, indicating that in addition to shallow-water environments, the Beipiao Formation also contains deep-water deposits, mainly lacustrine facies ranging from marshes to shore-shallow lakes and semi-deep lakes, albeit with a relatively limited extent (Fan, 2004; Zhen et al., 2016). They proposed that during the Early Jurassic, multiple lake basins existed in the Beipiao-Jinyang Basin, with strong separation between them. As research progressed, other scholars suggested that during the deposition of the Beipiao Formation in the Early Jurassic, the basin was a large lacustrine basin. The currently existing Nantianmen Fault Zone was only a latent fault within the basin before the end of the Early Jurassic. Since the Middle Jurassic, influenced by the Yanshanian movement, the Nantianmen Fault Zone gradually became active and developed into a significant uplift that divided the basin.

# 3 Dataset and methodology

This study utilizes data from three wells Bei M1, Beican 1, and Guan one in the Beipiao Basin; five wells LiaochaoD one and SZK01-04, as well as a long Kuntouyingzi outcrop section in the Jinyang Basin. The Kuntouyingzi outcrop, a long and well-exposed section in the basin center, provides a relatively complete stratigraphic record for this study. The LiaochaoD one well, located near the basin margin, was selected to represent the marginal depositional facies in the study area, while all other wells are situated in the basin center, reflecting the depositional facies in basin center. Integrating these data enables a comprehensive understanding of the lithology and depositional history of the Beipiao Formation across the study area. The primary focus is on the upper member of the Beipiao Formation, which predominantly consists of volcanic lava, volcanic breccia, tuff, thick mudstone, sandstone, and conglomerate. The thickness of this interval can exceed 800 m in the subsidence centers.

In this work we first classify the major lithofacies of the Beipiao Formation in the study area and then analyze the sedimentary processes and facies based on the lithofacies description. To elucidate the lithofacies types and sedimentary facies characteristics of the upper member of the Beipiao Formation in the Beipiao-Jinyang Basin, the following research methods were employed. (1) Core Observation and Description: Detailed descriptions of cores from the target interval of the Beipiao Formation were conducted. This included recording and analyzing typical sedimentary structures, photographing cores, and sampling for thin-section preparation. (2) Field Measured Section Analysis: The Kuntouyingzi outcrop section was investigated and measured in the field. Samples were collected for thin-section analysis. (3) Microscopic Thin-Section Observation: Thin sections were examined under an optical microscope to finely identify and classify the lithologies of the Beipiao Formation in the study area. We then examine the geochemical features of the black shale, e.g., the total organic carbon (TOC) and kerogen type, to explore the relationship between volcanic activity and depositional processes and the enrichment of organic matter in the black shale.

# 4 Lithofacies

Lithofacies (LF) are rocks or rock assemblages formed within a specific depositional environment, encompassing both the paleogeographic conditions of environment and the lithological characteristics of the sediments, which are fundamental blocks to interpret the sedimentary environment (Jiang et al., 2022a; Feng, 2022). Based on core observation, microscopic identification and assessment of volcanic clastic material input, terrigenous material input, and endogenous material (Liu et al., 2022; Jiang et al., 2022b; Ren, 2012), we have classified the lithofacies types of the Beipiao Formation in the Beipiao-Jinyang Basin into 13 categories (Table 1). The volcanic-related lithofacies classification follows the system proposed by Sun et al. (2001), which divides volcanic rocks into three main categories: pyroclastic lithofacies (volcanic clasts >90%), sedimentary pyroclastic clastic lithofacies (volcanic clasts 50%–90%), and pyroclastic sedimentary lithofacies (volcanic clasts 10%–50%). These lithofacies can be further subdivided into several subcategories based on grain size (e.g., coarse-grained: 0.1–2 mm; medium-grained: 0.01–0.1 mm; fine-grained: <0.01 mm), sedimentary structures (e.g., cross-bedding or planar bedding), lamination and grading (e.g., normal or inverse grading). Among these, volcanic clastic materials are various fragments formed during volcanic activity, collectively referred to as pyroclastics. The cement can be substances formed from the decomposition of volcanic ash or may be partially lava or terrestrial matrix.

## 4.1 Volcanic lava (LF1)

Rhyolite and basalt were primarily found in well SZK02, where volcanic lava deposits are relatively proximal to the volcanic crater. The volcanic lava is quite thin, indicating low volcanic activity intensity. The volcanic lava discovered mainly includes rhyolite and basalt. Rhyolite (Figures 3A–C) has a resorbed porphyritic texture, with the matrix exhibiting a felsitic texture composed of small felsic minerals and glass. Phenocrysts show resorbed edges and contain some pseudomorphs of primary crystals, as well as relicts and felsitic structures. The basalt (Figures 3D–F) in core samples appears gray-green, with a hyalopilitic texture. The matrix consists of early-crystallized pyroxene, which appears crystalline under crossed polarized light, with numerous feldspar grains present in the matrix. Phenocrysts show zoning textures.

## 4.2 Volcanic breccia (LF2)

Volcanic breccia is widely distributed, especially evident between 29.6 and 58.9 m in well SZK03 and 29–54 m in well SZK04. The volcanic breccia fragments are sub-angular, poorly sorted,

TABLE 1 Lithofacies classification of the beipiao formation in the beipiao-jinyang basin.

| No. | Lithofacies | Formation mechanism | Depositional environment |
|---|---|---|---|
| 1 | Volcanic Lava | Magma effusion | Volcanic crater |
| 2 | Volcanic Breccia | Volcanic debris flow | Near volcanic crater |
| 3 | Medium- to Coarse-grained Tuff | Medium to coarse volcanic density flow | Volcanic slope |
| 4 | Massive Fine-grained Tuff | Fine volcanic ash density flow | Semi-deep lake to deep lake |
| 5 | Laminated Fine-grained Tuff | Fine volcanic ash buoyant flow | Semi-deep lake to deep lake |
| 6 | Massive Tuffaceous Mudstone/Sedimentary Tuff | Fine volcanic ash density flow, mud gravity flow | Lake |
| 7 | Imbricated Conglomerate | Debris flow | Fan delta |
| 8 | Massive (Tuffaceous) Sandstone | Rapid deposition; sandy debris flow | Fan delta front, shallow lake, semi-deep lake |
| 9 | Massive Mudstone | Deep-water deposition | Deep lake |
| 10 | Normal Graded (Tuffaceous) Sandstone | Sandy turbidity flow, Ta segment; density flow | Semi-deep lake |
| 11 | Parallel-Laminated (Tuffaceous) Sandstone | Sandy turbidity flow, Tb segment | Semi-deep lake |
| 12 | Cross-Laminated (Tuffaceous) Sandstone | Sandy turbidity flow, Tc segment | Semi-deep lake |
| 13 | Deformed Sand-Mudstone | Slumping | Semi-deep lake |

and matrix-supported. The matrix consists of medium-to fine-grained tuff (Figure 3G). The volcanic breccia contains relatively small clastic particles, and the multiple depositional phases of volcanic breccia are interbedded with extensive black mudstone, indicating a distal deep-water depositional environment from the volcanic crater.

## 4.3 Medium to coarse-grained tuff (LF3)

Medium to coarse-grained tuff occurs in wells SZK02-04 and is deposited on volcanic slopes. Thin-section analysis reveals poorly sorted, sub-angular clastic grains with a clast-supported structure. The clasts are angular felsic crystal fragments, glass shards, and volcanic rock fragments, with feldspar grains often altered to carbonate particles. The interstitial material is tuffaceous, and there is an erosional contact with the underlying stratified sedimentary tuff (Figures 3H, I).

## 4.4 Massive fine-grained tuff (LF4)

Massive fine-grained tuff is widely developed in the study area, with tuffaceous content exceeding 50%. The massive tuff appears as massive gray-white material (Figure 4A). Under the microscope, crystal and glass shards are observed within a tuffaceous matrix, showing a matrix-supported structure. The crystal fragments are sub-angular to angular, poorly sorted, and small lenticular bodies are present, indicating turbulent water conditions during deposition (Figure 4F).

## 4.5 Laminated Fine-Grained Tuff (LF5)

Laminations usually consist of tuffaceous mudstone or sedimentary tuff interbedded with tuffaceous mudstone (Figures 4B, G). Within the laminated tuff, tuffaceous mudstone or sedimentary tuff forms mud clasts, showing weak basal scouring characteristics. The laminations exhibit gradual transitions between layers and are relatively rare in the study area.

## 4.6 Massive tuffaceous mudstone/sedimentary tuff (LF6)

The tuffaceous mudstone contains more than 50% mudstone or limestone components and is widely developed in the Kuntouyingzi area of the study region. The cores mostly exhibit a massive structure, and microscopic analysis reveals a complex composition including clay, carbonate grains, and tuffaceous material, with quartz crystal shards commonly present (Figure 4I). Under crossed polarized light, quartz grains show polycrystalline characteristics. Sedimentary tuff is characterized by high tuffaceous (>50%) content mixed with clay and carbonate grains, whereas tuffaceous mudstone has relatively lower tuffaceous content (<50%) and abundant crystal and glass shards (Figure 4H).

Pyroclastic rocks are well-developed in this region. Research indicates that the rapid burial of volcanic fine-grained materials is favorable for the preservation of organic matter (Liu et al., 2022). Volcanic activity plays an important role in the enrichment of organic matter (Lu et al., 2021), and the deep-sourced hydrothermal materials provided by volcanic processes are

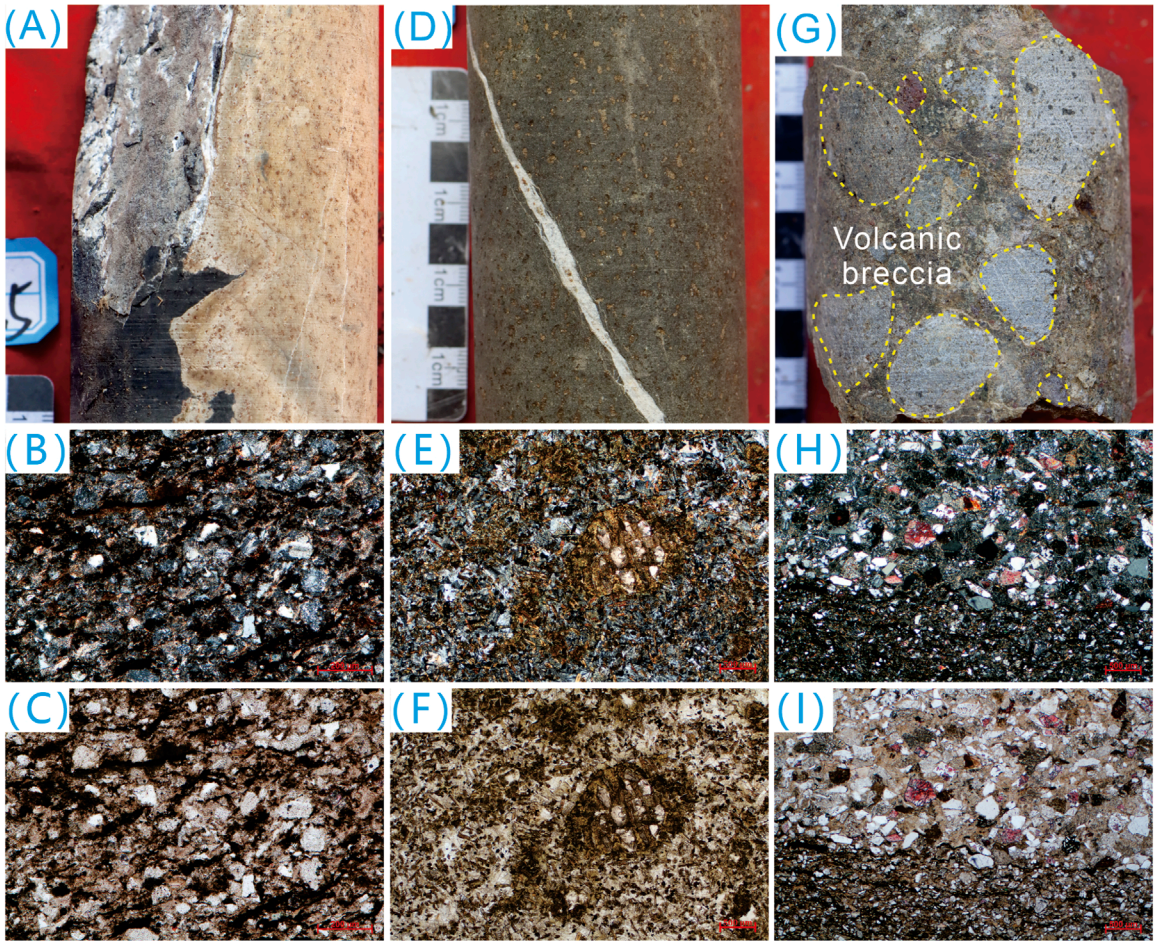


FIGURE 3
Features of Volcanic Lava, Volcanic Breccia, and Medium to Coarse-Grained Tuff. **(A)** Volcanic Lava - Rhyolite core, well SZK02, depth 296.05 m; **(B, C)** Rhyolite thin section under crossed polarized light and plane polarized light, well SZK02, depth 296.05 m; **(D)** Volcanic Lava - Basalt, well SZK03, depth 65.9 m; **(E, F)** Basalt thin section under crossed polarized light and plane polarized light, well SZK03, depth 65.9 m; **(G)** Volcanic Breccia core, well SZK03, depth 39.40 m **(H, I)** Medium to Coarse-Grained Tuff thin section under crossed polarized light and plane polarized light, well SZK02, depth 122.5 m.

crucial for hydrocarbon generation and reservoir improvement (Ren, 2012). The interbedding of organic-rich laminated mudstone and tuff, along with interlayer fractures, facilitates the migration of oil and gas. The presence of fine volcanic material positively impacts organic matter enrichment, hydrocarbon generation, and the conditions for oil and gas accumulation (Liu et al., 2022).

## 4.7 Imbricated conglomerate (LF7)

The imbricated conglomerate is mainly developed at well LiaochaoD one on the southeastern margin, belonging to marginal facies deposits. The clast diameters are mostly between 3–15 cm, poorly sorted, clast-supported, with clasts arranged in an imbricated fashion. The matrix is minor, gray to gray-white, but mostly reddish or red-brown (Figure 4C). The conglomerate composition is complex, indicating rapid fan delta deposition.

## 4.8 Massive tuffaceous sandstone (LF8)

Massive sandstone is developed at the top and bottom of the Beipiao Formation in the study area. The massive sandstone primarily consists of sandy material with a clastic (tuffaceous) structure and variegated fabric. The volcanic material typically results from pyroclastic deposits falling into a lacustrine basin, mixed with mud, gravel, and other sediments, and undergoing cementation and lithification. In the shallow drilled SZK01-04 cores, “mudstone rip-up clasts” or mudstone fragments with directional orientation can be seen (Figure 4D). In the Kuntouyingzi outcrop section, massive tuffaceous sandstone is observed (Figures 4L, M). Thin-section analysis shows fine-grained lithic sandstone with a clast-supported structure, where the clasts are mainly andesite or basalt rock fragments along with quartz grains. The quartz grains range from rounded to angular, suggesting a mix of terrigenous quartz and volcanic quartz crystals. The interstitial material is tuffaceous and carbonate (Figures 4J, K).

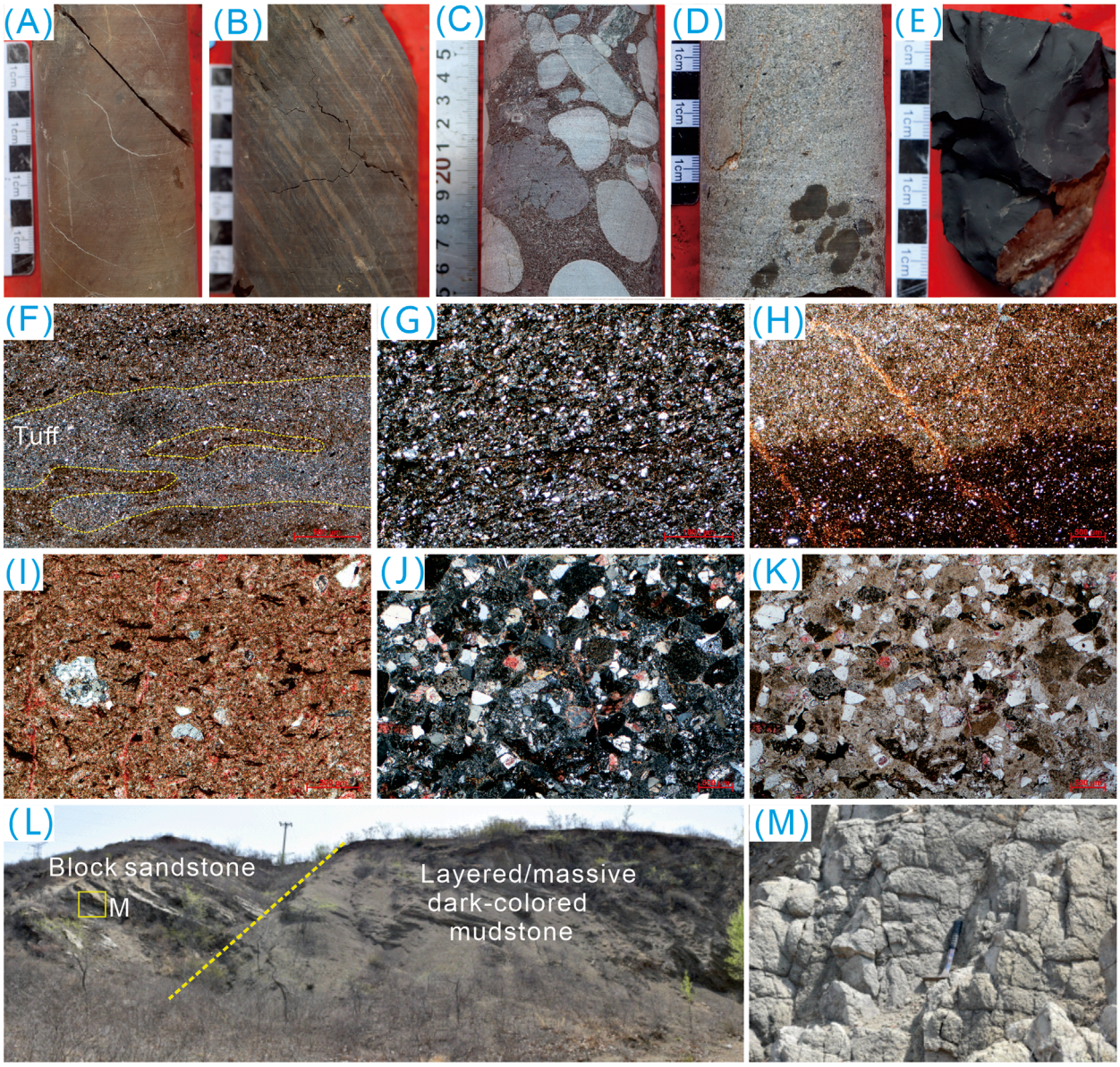


FIGURE 4
Features of Stratified/Massive/Striated Tuff, Stratified/Massive Tuffaceous Mudstone, and Conglomerate. **(A)** Massive Fine-Grained Tuff Core Photo, well SZK03, depth 57.02 m. **(B)** Laminated Fine-Grained Tuff, well SZK03, depth 39.05 m. **(C)** Conglomerate, well LiaochaoD 1, depth 857.6 m. **(D)** Massive Sandstone (with Mud Clasts), well SZK02, depth 131.5 m. **(E)** Black massive Mudstone, well SZK02, depth 222.85 m. **(F)** Laminated Fine-Grained Tuff, well SZK03, depth 39.05 m. **(G)** Glass Shard-Containing Tuff, thin section under crossed polarized light, well SZK02, depth 296.5 m. **(H)** Sedimentary Tuff/Tuffaceous Mudstone, thin section under crossed polarized light, well SZK02, depth 222.85 m. **(I)** Sedimentary Tuff, thin section under plane and crossed polarized light, well SZK03, depth 57.02 m **(J, K)** Massive (Tuffaceous) Sandstone, thin section under plane and crossed polarized light, well SZK02, depth 121.05 m. **(L)** Massive Sandstone and Bedded/Massive Mudstone, Kuntouyingzi outcrop. **(M)** Massive Sandstone, Kuntouyingzi outcrop.

## 4.9 Massive black mudstone/shale (LF9)

In the middle part of the Beipiao Formation in the Beipiao-Jinyang Basin, there is a substantial thick sequence of dark black mudstone. In the core samples, it appears as black and massive (Figure 4E), while in the Kuntouyingzi outcrop it is observed as bedded/massive black mudstone or shale (Figure 4L). The Beipiao Formation contains considerable thickness of black mudstone and shale, which can serve as a main hydrocarbon source rock.

## 4.10 Normal graded tuffaceous sandstone (LF10), parallel-laminated tuffaceous sandstone (LF11), cross-laminated tuffaceous sandstone (LF12)

These three lithofacies belong to the Ta, Tb, and Tc divisions of the Bouma sequence and are typically observed individually. In well SZK02, from 136.00 to 193.00 m, these features are evident. The Ta unit is represented by normal graded sandstone with mud clasts,

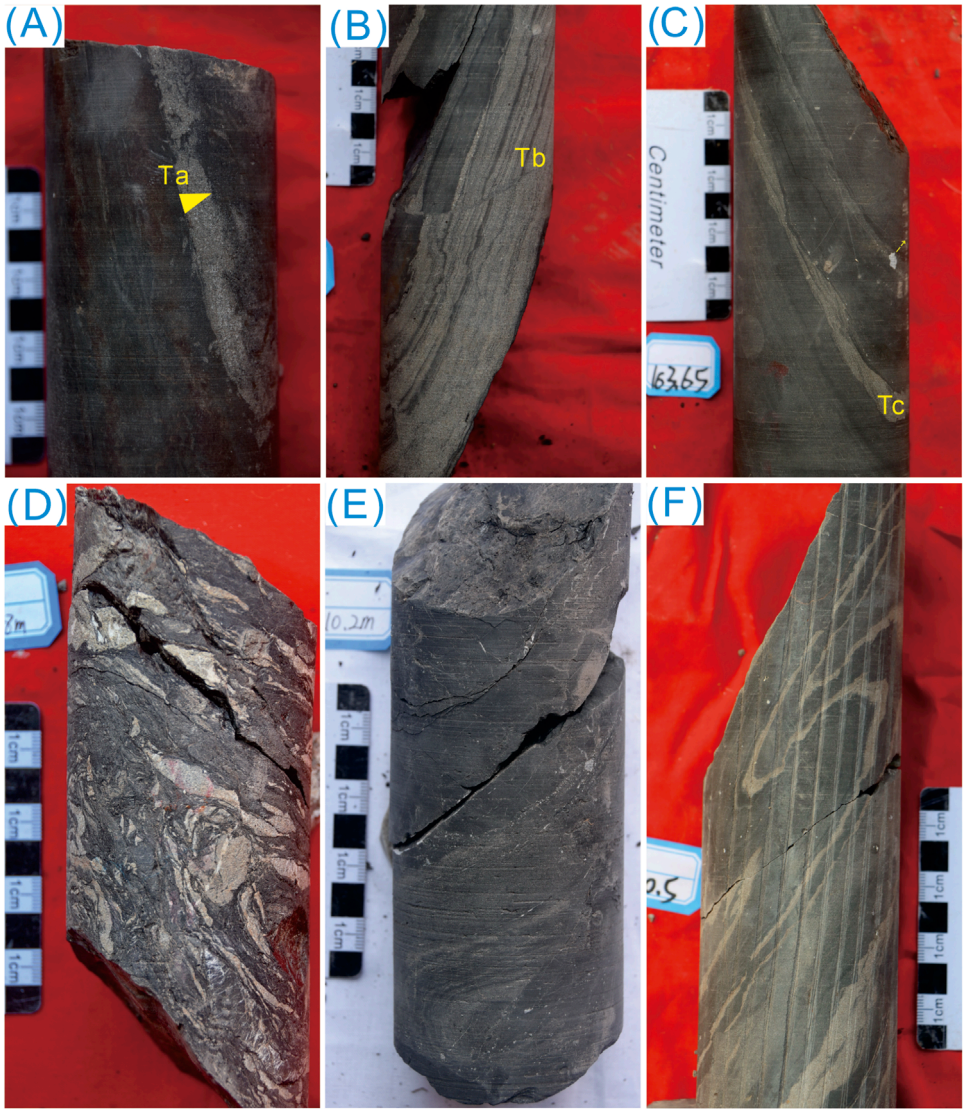


FIGURE 5
Characteristics of Normal Graded/Parallel-Laminated/Sand Grain Cross-Laminated (Tuffaceous) Sandstone and Deformed Sand-Mudstone. **(A)** Massive Tuffaceous Sandstone, well SZK02, depth 173.10 m. Ta-Turbidite Bouma sequence A; **(B)** Parallel-Laminated Tuffaceous Sandstone, well SZK02, depth 158.6 m. Tb- Turbidite Bouma sequence **(B, C)** Massive Tuffaceous Sandstone/Tuffaceous Mudstone, well SZK02, depth 163.65 m. Tc- Turbidite Bouma sequence **(C, D)** Slump Fold, well SZK02, depth 112.8 m. **(E)** Slump Fold, well SZK02, depth 210.2 m. **(F)** Slump Fold, well SZK02, depth 280.4 m. Please note the high dip angle of bedding in wells SZ01-SZK04 is not the depositional dip, instead it is caused by the titling of the strata due to the uplift.

erosional structures, load casts, and flame structures at the base of the layer (Figure 5A). The Tb unit consists of parallel-laminated sandstone (Figure 5B), while the Tc unit is characterized by siltstone with small ripples and deformation layers (Figure 5C), indicating gravity flow deposition in a deep-water environment with turbulent conditions.

## 4.11 Deformed Sandstone and mudstone (LF13)

Deformed sandstone and mudstone formed by slumping is widely developed in the deep-water area of the Beipiao-Jinyang Basin (Figures 5D, E). These rocks exhibit slump folding structures, reflecting the rapid depositional process of gravity flows. In well SZK02, slump-related sandstone and mudstones are developed, with sandy masses enveloped in mudstone (Figure 5E) and deformed lenticular sand bodies (Figure 5F). The mudstone is black to dark gray, indicating a deep to semi-deep lacustrine depositional environment at that time.

The 13 lithofacies classifications are building blocks that are then used to interpret sedimentary facies. Different facies combination can represent different sedimentary process and environment.

# 5 Sedimentary facies and environment

Based on field outcrops, core observations, lithofacies classification, and thin-section analysis, the depositional facies interpretation for the Beipiao Formation in the Beipiao-Jinyang Basin has been established. The study area is primarily characterized by fan delta facies, and lacustrine deposits, with subfacies including a shallow lacustrine subfacies between the fair-weather wave base and storm wave base, and a semi-deep to deep lacustrine subfacies below the storm wave base.

The shallow lacustrine subfacies include microfacies of fine-grained shallow lake deposits. The semi-deep to deep lacustrine subfacies consist of microfacies of fine-grained semi-deep to deep lake deposits, gravity flow deposits, and volcaniclastic deposits. On the southeastern margin of the basin, fan deltas are well developed, mainly characterized by braided channel deposits of fan delta plain and fan delta front.

## 5.1 Shallow lake

### 5.1.1 Fine-grained shallow lake deposits microfacies

The lithology of fine-grained shallow lake deposits mainly includes mudstone (LF6), silt-bearing mudstone, and siltstone, typically dark gray in color. Bioturbation features are visible (Figures 6A, B), with thin siltstone layers often present. The mudstone may have been deposited under slack water conditions during fair weather, while the thin sandy layers (Figure 6C) have diverse origins, primarily resulting from the reworking of delta-derived sediments by wave action.

## 5.2 Semi-deep to deep lacustrine subfacies

### 5.2.1 Tempestite microfacies

Core observations from the wells in the Beipiao-Jinyang Basin indicate the presence of storm deposits within the Beipiao Formation. These deposits are characterized by siltstone, silty sandstone, and fine sandstone, with few muddy siltstone containing mud clasts. The deposits commonly display an inverse-to-normal grading sequence or a normal grading similar to Bouma sequences. The mudstone is gray-green to dark gray, suggesting a reducing environment. Typical storm-related structures include hummocky cross-stratification (Figures 6D, E), mudstone rip-up clasts, and gutter casts (Figure 6F), as well as wavy bedding (Figure 6G) and lenticular bedding (Figure 6I). Deformation features such as load casts and fold deformations are also present (Figure 6F). Massive sandstone indicative of rapid deposition is also observed, along with bioturbation features (Figure 5H).

### 5.2.2 Deep-water gravity flow microfacies

This study uses a classification scheme for sediment gravity flows based on sedimentary processes and rheology proposed by previous researchers' work (Pan, et al., 2017; Zavala and Pan, 2018). Core observations reveal that the gravity flow deposits in the Beipiao Formation of the Beipiao-Jinyang Basin include slumping deposits, sandy debris flows, and turbidites, with sandy debris flows and turbidites being the most common.

The sandy debris flow deposits in the Beipiao Formation mainly consist of siltstone, massive fine-grained sandstone (LF8), and muddy siltstone, with occasional conglomerates. Slumping deposits, originating from thin interbedded siltstone and mudstone, exhibit thin sandstone layers that form convoluted and faulted structures called sand pillows (LF13). The interiors of sand pillows display inclined "S"-shaped convoluted laminations, or the pillows themselves may fold into horizontal or inclined "S"-shaped irregular sand bodies, with some forming slump folds (Figures 7A–C). Sandy debris flow deposits in the region often contain poorly sorted shell fragments. Other sedimentary structures observed in sandy debris flow deposits include groove casts, gutter casts, load casts, liquefaction cones, subaqueous dikes, and escape structures. These deposits are found in wells SZK01-04 (Figures 7D–H).

Turbidite deposits are also widespread in the Beipiao Formation, typically with sand bodies less than 1 m thick, and often even less than 0.1 m, indicating frequent turbidite events (LF11 and 12). The turbidite lithology mainly consists of siltstone, fine sandstone, and muddy siltstone, with occasional conglomerates. Turbidite deposits are characterized by graded bedding (LF10) (Figure 7I), with the tops of graded beds showing small-scale parallel laminations (LF11) (Figure 7L), cross-laminations (LF12), and ripple cross-laminations (generally less than 10 cm thick) (Figure 7J). Groove casts and gutter casts are commonly found at the base, and liquefaction features are often seen within the deposits (Figures 7E, K).

### 5.2.3 Pyroclastic microfacies

Core and thin-section observations from the Guan one well (depth 400–550 m) in the Beipiao Basin reveal that the Beipiao Formation contains significant amounts of pyroclastic material. These contemporaneous volcanic clasts (lithic fragments, crystal shards, and glass shards) were transported by air or water into the lake basin, where they were deposited and consolidated. The deposits primarily consist of tuffaceous siltstone and thin tuff layers, ranging from centimeters to micrometers in thickness (Figure 8A). The tuffaceous siltstone displays characteristics of volcanic density currents (Figure 8B). Thin layers of tuff, often in micrometer scale, are typically in abrupt contact with dark mudstone or oil shale, indicating a deep-water stagnant depositional environment (Figures 8C, D). The tuff layers contain abundant volcanic glass but relatively few crystal shards, and they exhibit horizontal and massive bedding structures (Figure 8E).

In wells SZK01-04, several layers of volcanic breccia were found. These breccias are characterized by composite volcanic clasts within a matrix-supported tuff. The tuff is rich in crystal fragments, while the clasts are sub-angular to angular. The clast sizes vary from a few millimeters to several centimeters, with the most developed layers observed in well SZK04, suggesting strong volcanic influence in proximity to the volcanic source.

### 5.2.4 Semi-deep to deep lacustrine fine-grained sedimentary microfacies

The semi-deep to deep lacustrine fine-grained microfacies is extensively developed and represents the primary depositional facies type of the Beipiao Formation in the Beipiao-Jinyang

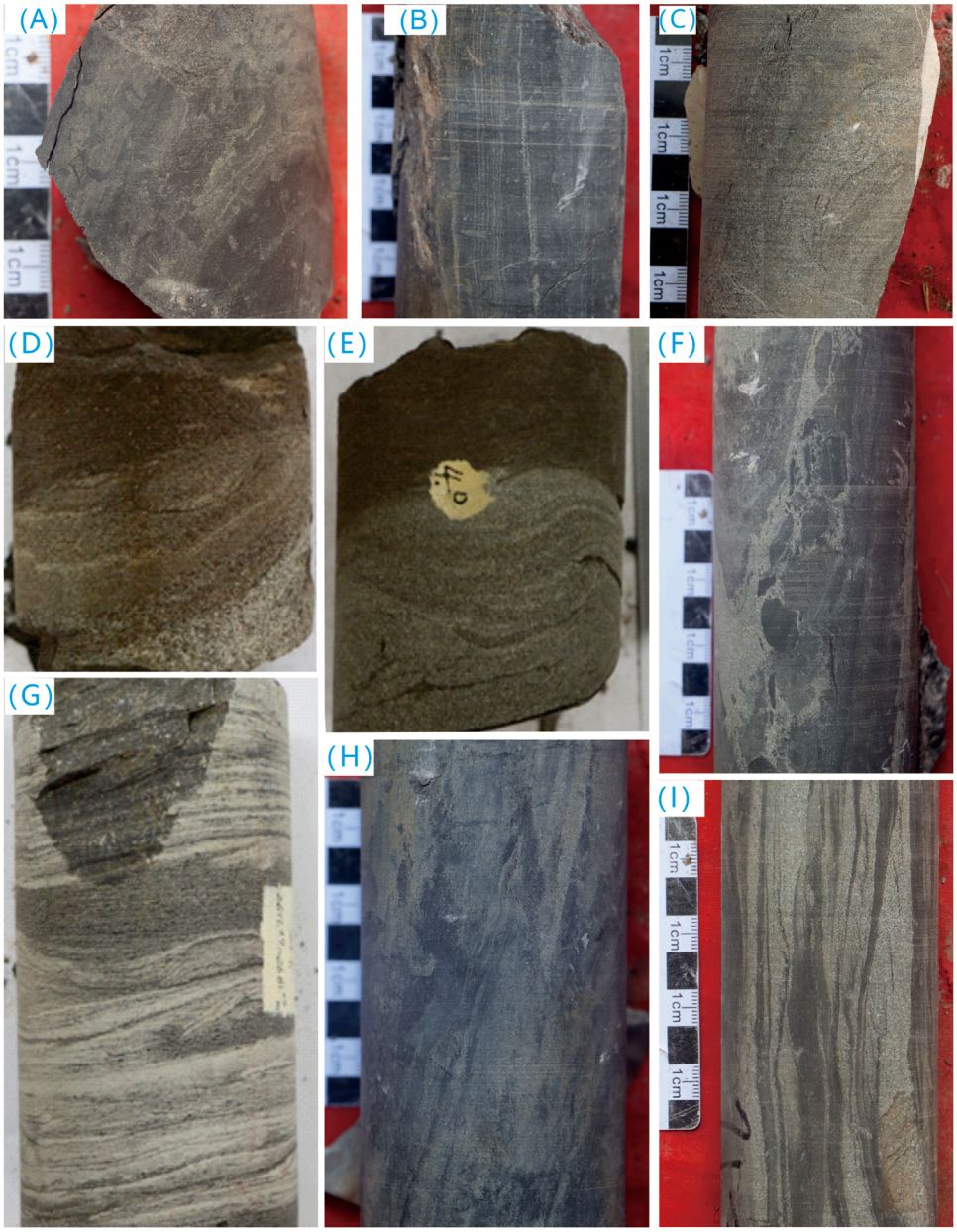


FIGURE 6
Typical Facies characteristics of Storm s and Shallow Lake Fine-Grained deposits. **(A)** Mudstone with thin siltstone layers, extensive bioturbation with visible burrows, well SZK 03, depth 155.20 m. **(B)** Mudstone with millimeter-scale thin siltstone layers, visible bioturbation, well SZK 03, depth 231.80 m. **(C)** Muddy siltstone, well SZK04, depth 79.55 m. **(D)** Storm truncation structure, trough cross-stratification, well Guan 1, depth 399.8 m. **(E)** Deformation and truncation structure, well Guan 1, depth 426.2 m. **(F)** Basal scour with retained mud clasts arranged in a v shape, well SZK 03, depth 254.2 m. **(G)** Hummocky cross-stratification in microcrystalline limestone, well Beican 1, depth 2,677.4 m. **(H)** Bioturbation structure, well Szk03, depth 259.90 m. **(I)** Wavy bedding, well SZK03, depth 212.5 m.

Basin. The lithology of these deposits is dominated by mudstone or, which appears dark gray to black and mostly occurs as massive deposits (LF4, 5, six and 9; Table 1) (Figure 8F). Laminated black mudstone and shale deposits are both observed in outcrop section and core (Figure 8G), and the accumulated thickness is significant, indicating a deep-water semi-deep to deep lacustrine environment. In the Beipiao-Jinyang Basin center, the total mudstone thickness can exceed several hundred meters.

## 5.3 Fan delta

The fan delta facies is primarily observed in well LiaochaoD 1. In this location, the lithology of the Beipiao Formation consists mainly of extensive conglomerate beds interbedded with medium to coarse-grained sandstone containing lithic feldspar. Some layers are cemented with tuffaceous material, and no typical Beipiao Formation fine-grained shale strata are observed, indicating the development of the fan delta.

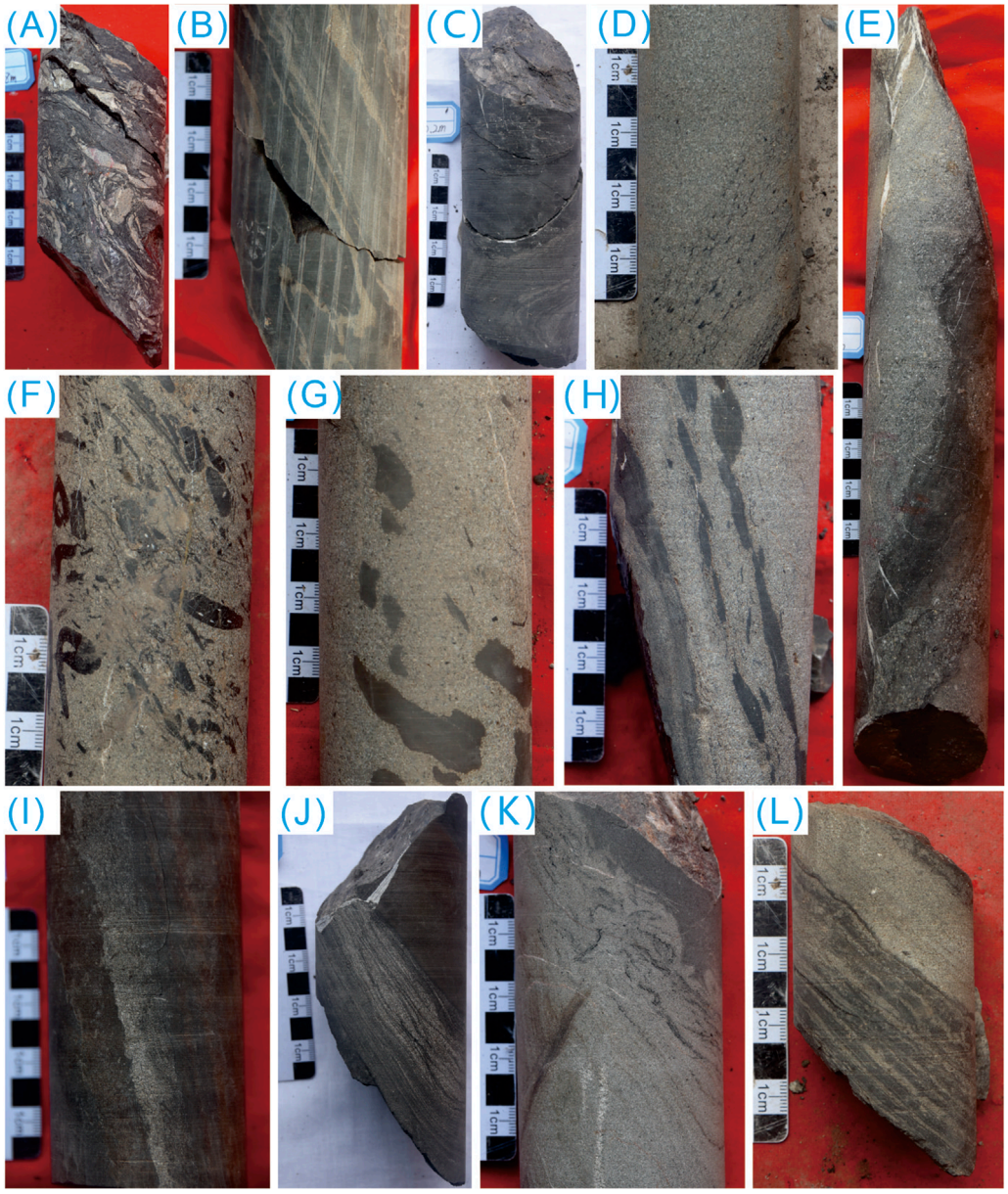


FIGURE 7
Typical characteristics of deep-water gravity flow sedimentary microfacies. **(A–C)** Slumping Deposits, Slump Structures, well SZK02. **(D)** Sandy Debris Flow Deposit, Massive Sandstone with Millimeter-Scale Mudstone Clasts, well SZK01, depth 252.8 m. **(E)** Turbidite Ta Unit, well SZK02, depth 197 m. **(F)** Sandy Debris Flow Deposit, Chaotically Distributed Mud Clasts, well SZK01, depth 252.18 m. **(G)** Sandy Debris Flow Deposit, Chaotically Distributed Mudstone Fragments, well SZK02, depth 303.37 m. **(H)** Sandy Debris Flow Deposit, Mud Clasts Aligned Along Bedding, well SZK02, depth 129.6 m. **(I)** Turbidite Ta Unit, well SZK02, depth 173.1 m. **(J)** Turbidite Tc Unit, Sand Laminations, well SZK02, depth 211.3 m. **(K)** Turbidite Ta-Tb Unit, Basal Load Cast with Liquefaction Features, well SZK02, depth 170.4 m. **(L)** Turbidite Tb Unit, Parallel Laminations, well SZK01, depth 254.95 m.

The braided channel of the fan delta plain exhibits imbricated gravel deposits and massive conglomerates (Figure 9A). In some areas, the gravels display an oriented arrangement (Figures 9B, C), and at the contact between gravel and sand, a clear scour-and-fill structure is observed, indicating erosional contacts (Figure 9D). Due to strong hydrodynamics, the matrix is mainly composed of medium-grained sandstone rather than mudstone. The conglomerates are dispersed within the sandy matrix, indicating rapid deposition. Furthermore, the varied grain sizes of the conglomerates and poor sorting suggest a quick unloading of sediments. The braided channel of the fan delta front is characterized by sandy deposits with cross-bedding, and no mudstone or siltstone is present.

The fan delta deposits can also be observed on the Kuntouyingzi outcrop when the lake level low and the fan delta can prograded into the center of the lacustrine basin. It is mainly characterized by thick and massive conglomerate and sandstone on the outcrop (Figure 10).

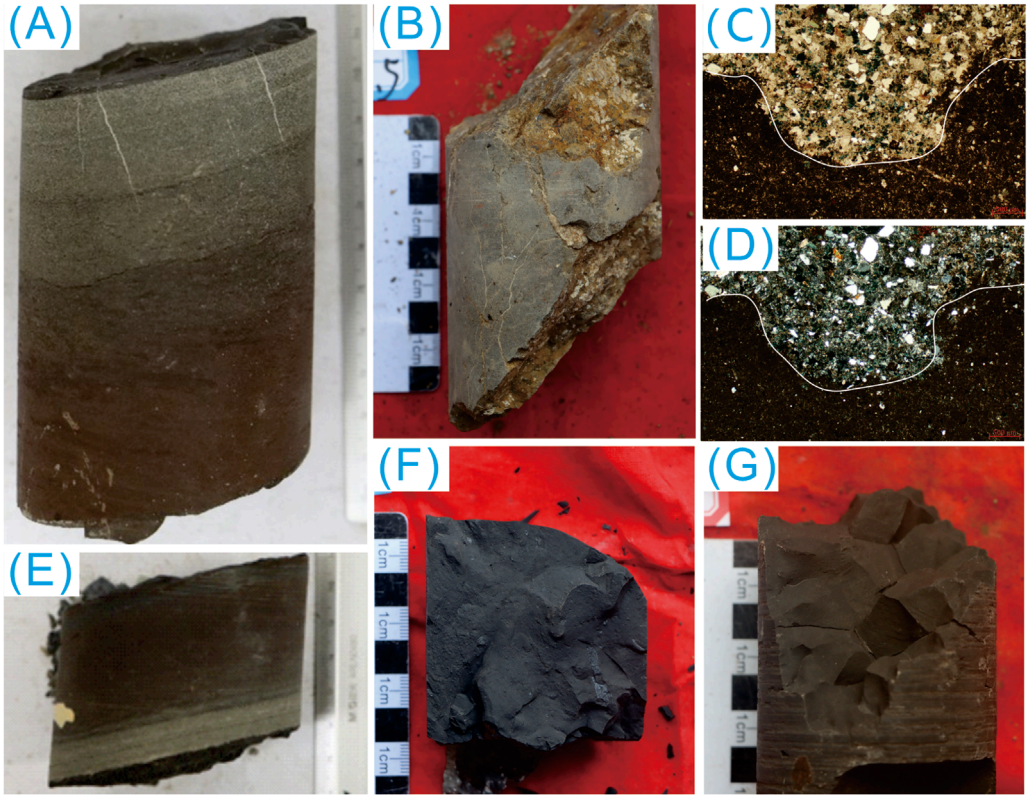


FIGURE 8
Pyroclastic sediments and semi-deep-deep lake fine-grained sedimentary characteristics. **(A)** Massive Tuff, well Guan 1, depth 424.1 m. **(B)** Massive-Bedded Tuff, well SZK04, depth 35.50 m **(C, D)** Volcanic Lithic Fragments, Groove Casts (under plane and crossed polarized light), well Guan 1, depth 464 m. **(E)** Massive Mudstone and Parallel-Laminated Tuff, well Guan 1, depth 418.3 m. **(F)** Dark Gray Massive Mudstone, well SZK02, depth 253.15 m. **(G)** Dark Gray Massive Mudstone, well SZK03, depth 344.8 m.

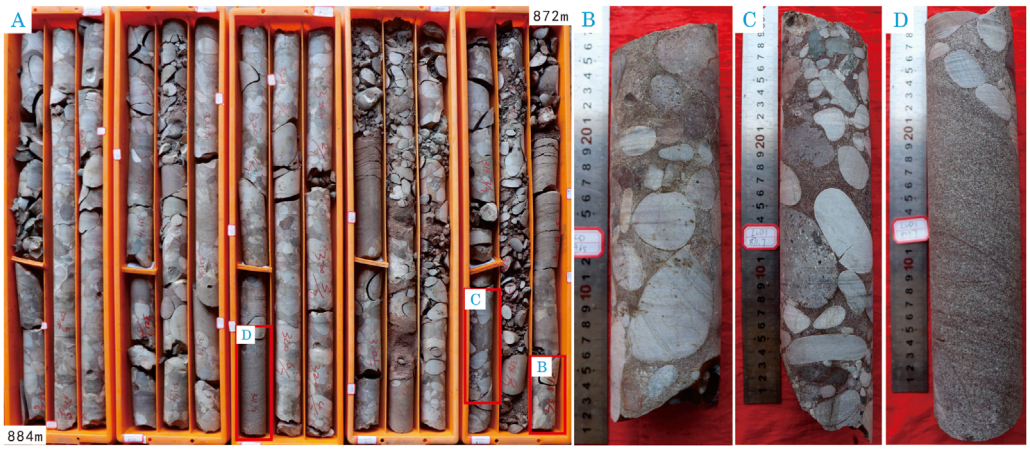


FIGURE 9
Typical characteristics of fan delta sedimentary facies. **(A)** Core Box Photo, red box indicates red-brown sandstone, well LiaochaoD 1, depth 884–872 m. **(B)** Conglomerate with grain size 2–10 cm, well LiaochaoD 1, depth 869.65 m. **(C)** Conglomerate with oriented arrangement of gravel, well LiaochaoD 1, depth 871.7 m. **(D)** Red-brown sandstone with developed scour surfaces and cross-bedding, well LiaochaoD 1, depth 877.7 m.

## 5.4 Vertical sedimentary facies evolution

Based on lithofacies and sedimentary facies analysis, the sedimentary environment of the Jurassic Beipiao Formation can be interpreted from its basal to upper sections (Figure 10). The Kuntouyingzi outcrop offers a continuous and well-exposed view of the Beipiao Formation, including its unconformable contact with the underlying Neoproterozoic Wumishan Formation dolomite (Figure 10A). Although portions of the basal and upper sections of the Beipiao Formation are missing at

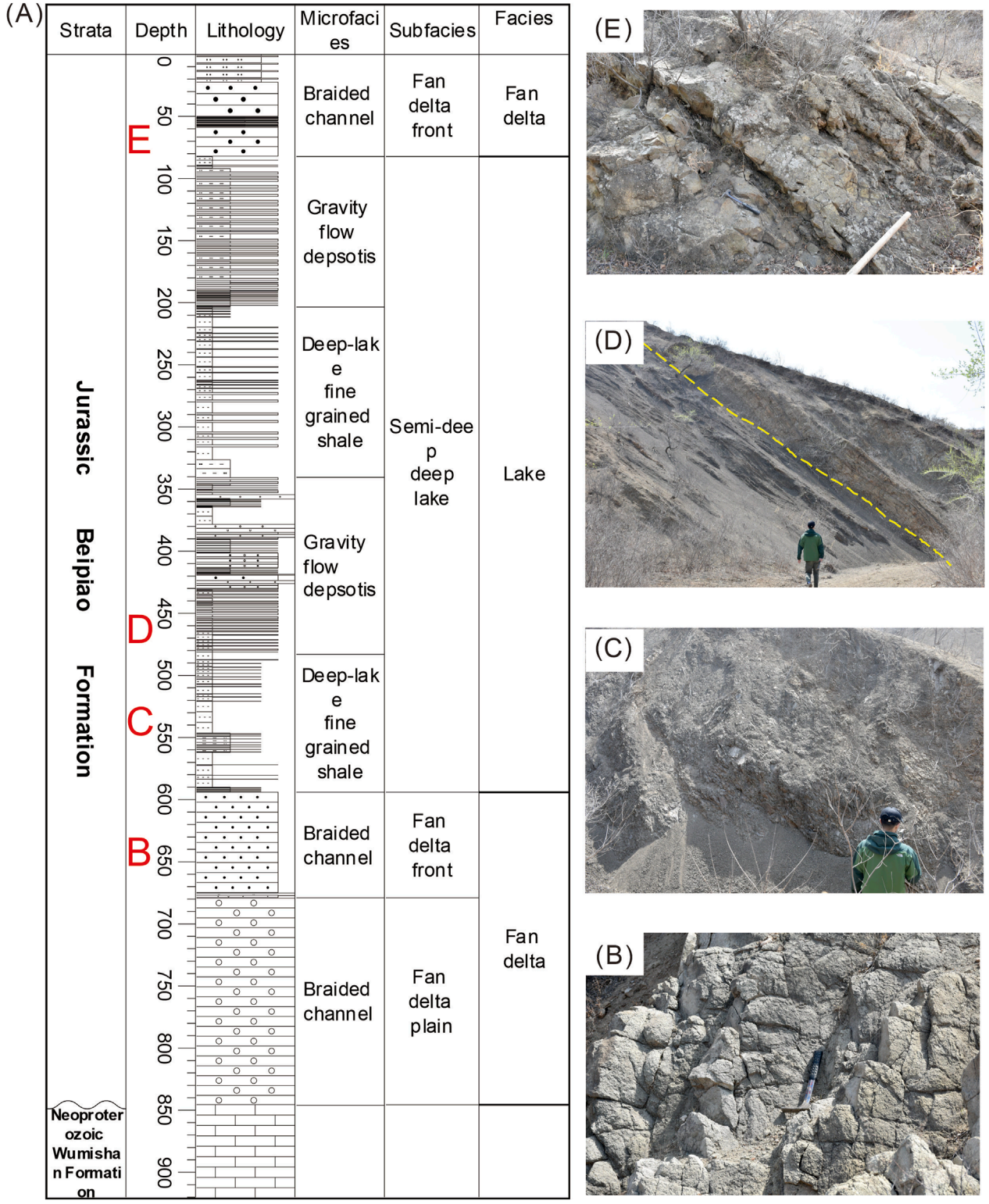


FIGURE 10
**(A)** The sedimentary facies and environment evolution from basal to top of the Beipiao Formation, Kuntouyingzi outcrop. **(B–E)** is the photo location.

this location, the approximately 900-m-thick exposed outcrop effectively represents the sedimentary characteristics of the formation.

The lower part of the Beipiao Formation is dominated by massive conglomerates and thick to medium-grained sandstones, indicative of a fan delta depositional environment (Figure 10B). The

fan delta facies is commonly developed along the basin margin. Well Liaochaodi one is located on the eastern basin margin and shows a continuous and long interval of conglomerate, indicating strong hydrodynamics. The high dipping angle of conglomerates indicates they are deposited in a steep slope, likely suggesting a depositional environment of fan delta near the sediment source. Due to its proximity to the basin, the Well Liaochaodi one is dominated by fan delta facies in the whole Beipiao Formation. The middle section of Kuntouyingzi outcrop is primarily composed of thick shale, interbedded with thin sandstone or pyroclastic deposits, characteristic of deep-water fine-grained sediments and gravity flow deposits (Figures 10C, D). Such fine-grained lithologies characterized by thick shale or turbidite Bouma sequence are also common in wells SZK01-04 (see Figure 1 for location; Figures 6–8). During this period, the lake expanded, reaching its maximum depth. The upper part of the Beipiao Formation transitions back to coarse-grained sandy deposits, reflecting the progradation of the fan delta into the lake (Figure 10E). These lithological changes represent a complete sequence cycle: an initial low lake level followed by transgression, culminating in a stable highstand lake level.

The facies evolution aligns with regional geological history. Previous studies indicate that the Beipiao Formation is influenced by the Yanshan orogenic event (Sun QS. et al., 2019). Following the volcanic eruption of the Xinglonggou Formation, the basin began to rift, leading to the deposition of relatively coarse-grained fan and alluvial delta facies. As rifting continued, the basin area expanded, and lake depth increased, favoring the development of deep-lake environments. Subsequently, as basin extension slowed, deltaic facies began to prograde into the basin center, which corresponds to the coarse-grained deposits in the upper part of the Beipiao Formation. Later, the basin was filled by another pulse of volcanic activity, resulting in the formation of Haifanggou-Tiaojishan pyroclastic deposits (Wang, 1993; Sun S. L. et al., 2019).

## 5.5 Sedimentary facies spatial distribution characteristics

Based on the lithofacies and sedimentary facies analyses, as well as the thickness map of the Beipiao Formation in the study area (Figure 11), a spatial facies distribution can be obtained. During the deposition of the Beipiao Formation in the Beipiao-Jinyang Basin, alluvial fan and fan delta deposits developed in the eastern and southern parts of the basin. These deposits, characterized by limited sandbody extension and distribution (Figure 12), were the primary sources of terrigenous clastic input, with well LiaochaoD one serving as the key representative. In the eastern parts of Batuying and Ershijiazi towns, shore-shallow lake and storm deposits are primarily developed. The shore-shallow lake deposits cover a relatively small area and are generally distributed in a northeast-southwest elongated pattern.

In the northwest part of the basin, west of Jinlingsi and Yangshanzhen, semi-deep to deep lacustrine deposits are extensively developed. Volcanic deposits are frequently observed in the Kuntouyingzi area, represented by wells SZK01-04 and Bei M1. Along the northern margin of the Beipiao Basin, small nearshore subaqueous fans have developed, which also evolved into semi-deep to deep lacustrine deposits, with wells Guan one and Beican one serving as representative wells in this region.

In general, the Beipiao Formation in the study area is characterized by fan delta deposits at the basin margin and widespread deep-lake environments in the basin center, with fan delta fronts and shallow lakes developed in between. The deep-lake facies are predominantly found in the middle part of the Beipiao Formation, while the lower and upper parts are dominated by fan delta and braided delta deposits.

# 6 Geochemical characteristics of source rocks

A total of 209 data samples were collected for this study, including 170 drilling core samples and 39 field outcrop samples. The data mainly includes five organic geochemical analyses, such as total organic carbon (TOC) and pyrolysis. Of the samples, 200 are from the Jinyang Basin and nine are from the Beipiao Basin. The samples were taken from wells SZK01, SZK02, SZK03, and Guan 1, as well as outcrops at Xiaogangou, Wolong, Dajingou, Shimen Gou, Dongkuntouyingzi, Shimen Gou Village, and Nanyao Village.

## 6.1 Organic matter abundance

Organic matter abundance is the material basis for evaluating source rocks, and commonly used indicators for assessing the organic matter abundance in source rocks include total organic carbon (TOC%), chloroform "A," total hydrocarbons (HC), and pyrolysis hydrocarbon potential (S1+S2). Analysis of these indicators reveals variability in organic matter abundance across different wells and outcrops. Well SZK02 has the highest organic matter abundance, followed by well SZK03 and the Shimen Gou outcrop in Changbaoyingzi Township. The Wolong, Nanpiao Yanjialing, and Diaojiagou outcrops in Batuyingzi Township exhibit the lowest values, with average indicator values far below the average for the Jinyang Basin.

The TOC content of core and field-measured outcrop samples ranges from 0.16% to 14.2%, with an average of 1.89% (Figure 13A). Only five samples have a TOC content below 0.4%; two samples fall between 0.4% and 0.6%; 32 samples are between 0.6% and 1.0%; 86 samples, accounting for 46%, are between 1.0% and 2.0%; and 62 samples, accounting for 33.15%, have TOC values greater than 2.0%. These results indicate that the mudstone in the Beipiao Formation generally represents moderate to good source rock, with very few poor or non-source rock samples.

The chloroform "A" content in core samples ranges from 0.0030% to 0.3072%, with an average of 0.0846% (Figure 13B). Seven samples have a chloroform "A" content below 0.015%; 30.52% of the samples are between 0.015% and 0.050%; 34.42% are between 0.050% and 0.100%; 25.32% are between 0.100% and 0.200%; and eight samples have values greater than 0.200%. These indicators consistently suggest that the Beipiao Formation source rocks are mainly moderate to good in terms of organic matter abundance.

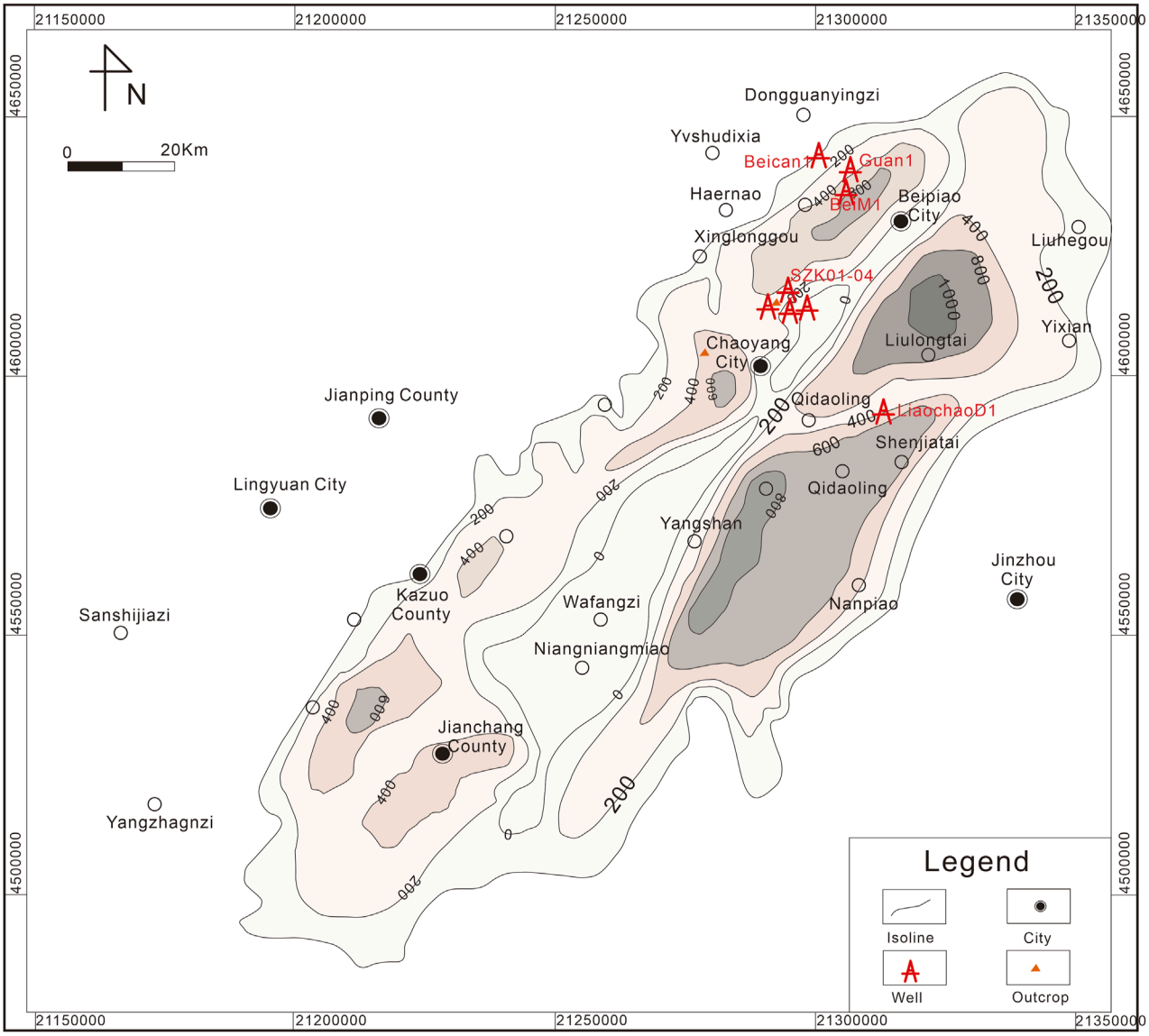


FIGURE 11
Strata thickness map of the Beipiao Formation in the Western Liaoning.

## 6.2 Organic matter types of source rocks

The organic matter type of the Beipiao Formation source rocks in the study area was analyzed using the pyrolysis parameters IH (hydrogen index) and IO (oxygen index). In the organic matter type identification diagram (Figure 13D), most of the sample points fall in the Type II region, with only a few in the Type III region. Therefore, it is concluded that the organic matter in the Beipiao Formation source rocks is predominantly Type II, which leans toward humic-sapropelic. This indicates that the hydrocarbon precursors mainly originated from lower aquatic organisms and higher plants, with a greater contribution from higher plants.

The cross-plot of HI *versus* Tmax for the Beipiao Formation source rock kerogen (Figure 13D) suggests that it generally belongs to a mixed organic matter type, making it challenging to accurately identify. This also indicates that the Beipiao Formation source rocks are in a high to over-mature stage. It can be observed that the kerogen from wells SZK02 and SZK03 has reached an over-mature stage, making its type difficult to distinguish. The kerogen in field outcrops is primarily of Type II2, while the kerogen in well Guan one mainly falls between Type II1-II2 and Type II2.

## 6.3 Organic matter maturity

Comparing the Wolong and Kuntouyingzi sections, although both have relatively high residual organic carbon, the Wolong section shows extremely low hydrocarbon potential (S1+S2). The vitrinite reflectance (Ro) measurements (Figure 13F) indicate that the samples from the Wolong section generally have Ro values greater than 1.5%, with higher values found closer to the diorite

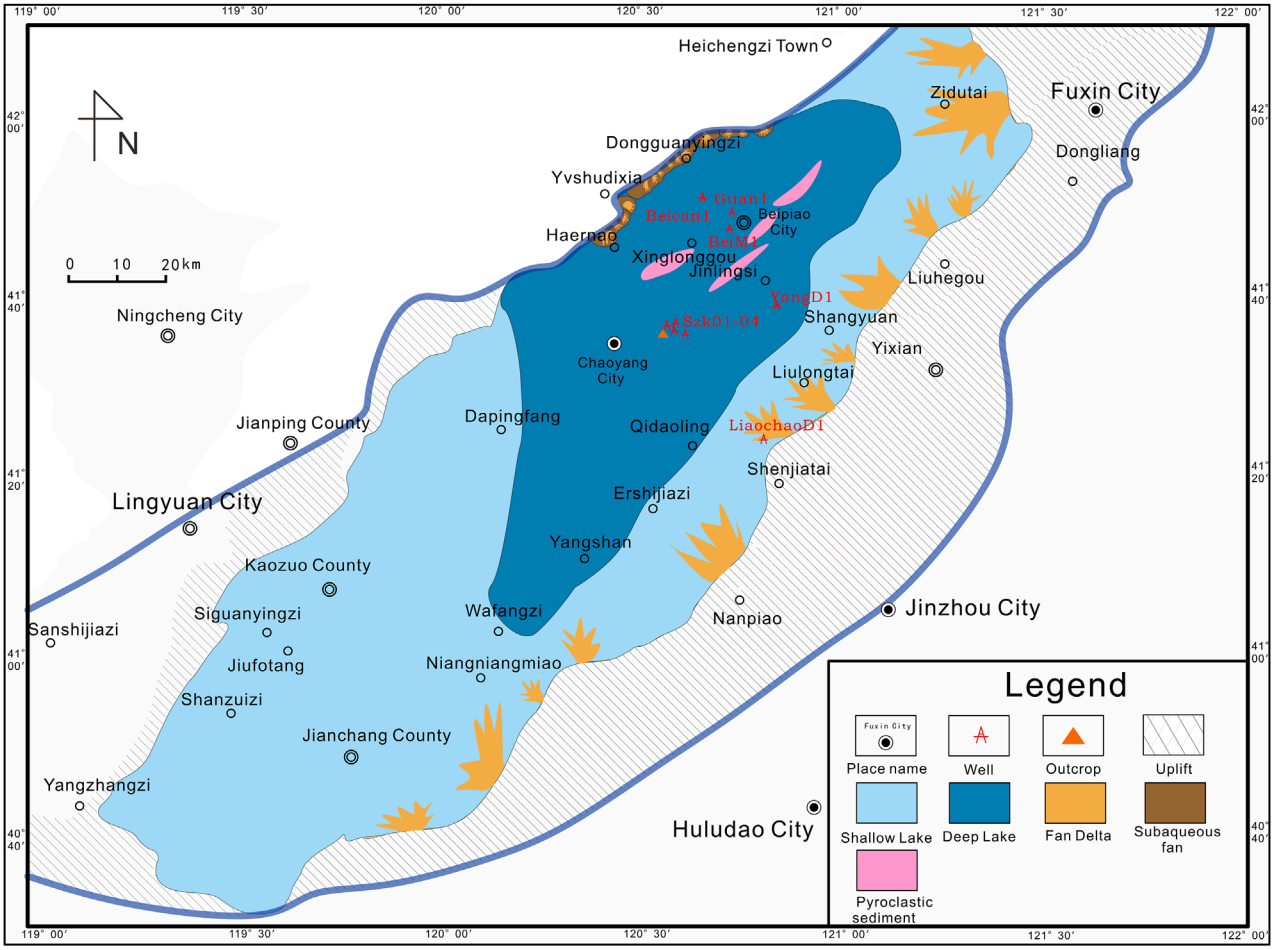


FIGURE 12
Spatial sedimentary facies distribution in the lower jurassic beipiao formation of the beipiao-jinyang basin, western liaoning.

porphyry dike, reflecting thermal alteration of the source rock by the intrusive body.

Based on organic matter abundance and distribution data, as well as Tmax distribution (Figure 13E) and the cross-plot of Production Index (PI) *versus* Tmax (Figure 13C), it is observed that Tmax is positively correlated with vitrinite reflectance (Ro). Typically, Tmax greater than 435°C is considered indicative of a mature stage, whereas Tmax below 435°C indicates an immature stage. For the Beipiao-Jinyang Basin samples, most of the Tmax values fall within the range of 445°C–480°C, indicating a mature stage. The PI *versus* Tmax cross-plot shows that the thick mud-shale layers in wells SZK01-04, located at the center of the basin, are in the later stage of the oil-generation peak and have reached a high maturity to over-mature stage suitable for gas generation. In contrast, shallower areas closer to the basin margins are currently in the oil-generation stage.

It can be concluded that the Lower Jurassic Beipiao Formation in the Jinyang-Beipiao Basin has potential source rocks that are at the mature stage and have reached the oil-generation peak. Although the sample data are from outcrop-controlled areas influenced by faulting and thrust structures, which are unfavorable for hydrocarbon preservation, recent seismic exploration results indicate that beneath the large volcanic clastic rock coverage of the Yixian and Tiaojishan Formations on the eastern side of the basin, there are still substantial deposits of the Beipiao Formation. The hydrocarbon source rocks in these regions are well-developed, showing similar or even better characteristics compared to the existing data, and the two regions are interconnected.

# 7 Discussion

## 7.1 Depositional environment

Previous studies have considered the Beipiao Formation in western Liaoning as a set of coal-bearing strata, suggesting an overall shallow-water environment (He et al., 2006; Wang, 2011). However, some researchers have observed gray-black sandstone, mudstone, and shale in core samples, indicating that in addition to shallow-water environments, the Beipiao Formation also contains certain deep-water deposits, mainly lacustrine facies ranging from marshes to shore-shallow lakes and semi-deep lakes, albeit with a relatively limited extent (Fan, 2004; Zhen et al., 2016). They proposed that

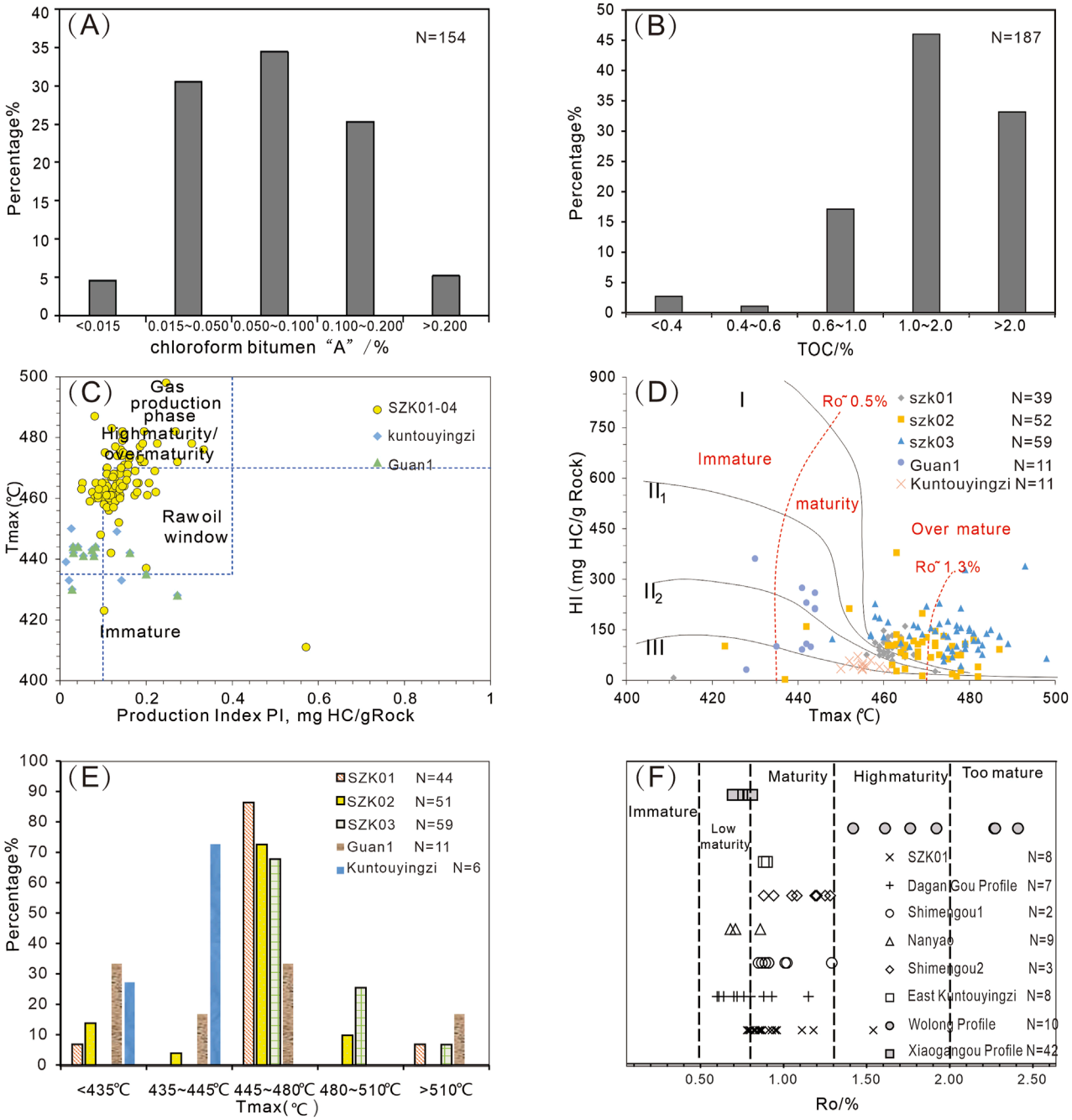


FIGURE 13
Geochemical features of the source rocks of the Beipiao Formation in the Western Liaoning. **(A, B)** Histogram of Organic Matter Abundance; **(C)** Cross plot of the PI and Tmax; **(D)** Organic matter types and source rock maturity; **(E)** Kerogen maturity based on Tmax data; **(F)** Distribution map of vitrinite reflectance ($R_0$). Some of the organic data was collected from published articles (Sun QS. et al., 2019; Zhen et al., 2016; He et al., 2006; Zhang et al., 2017a; Sun et al., 2017a; Fan, 2004).

during the Early Jurassic, multiple lake basins existed in the Beipiao-Jinyang Basin, with strong separation between them. As research progressed, other scholars suggested that during the deposition of the Beipiao Formation in the Early Jurassic, the basin was a large lacustrine basin. The currently existing Nantianmen Fault Zone was only a latent fault within the basin before the end of the Early Jurassic. Since the Middle Jurassic, influenced by the Yanshanian movement, the Nantianmen Fault Zone gradually became active and developed into a significant uplift that divided the basin.

In this study, wells from the Beipiao Basin (wells Bei M1, Guan1, and BeiCan 1) and the Jinyang Basin (wells SZK01, SZK02, SZK03, and SZK04) are characterized by thick black mudstones in the middle of the Beipiao Formation, indicating a semi-deep to deep lake environment. The storm deposits observed on cores also

indicate a relative deep lake level that below the storm wave base. The abundant gravity flow deposits in the middle part of the Beipiao Formation further support a deep-water environment. Additionally, the Kuntouyingzi outcrop contains approximately 300 m of thick black shale interbedded with thin gravity flow deposits, suggesting a deep-water setting. Regional strata thickness mapping (Lee et al., 2018) shows extensive Beipiao strata distribution in western Liaoning (Figure 11), verifying that the Jinyang, Beipiao, and Jianchang-Kazuo Basins (locations shown in Figure 1) were part of a single large basin during the depositional period of the Beipiao Formation.

Overall, drilling data and outcrop observations in the basin center, along with the strata thickness map, indicate the presence of a widely developed deep-water environment in the middle Beipiao Formation across western Liaoning. The only exception is the LiaochaoD one well, located at the basin margin, which displays conglomerate and coarse-grained deposits indicative of fan delta deposition (Figure 9). These findings provide additional evidence that the Jurassic Beipiao Formation in western Liaoning was deposited in a large, deep-water basin. More importantly, these findings suggest that the organic-rich black shale development has been largely underestimated. Continued exploration has also led to the discovery of hydrocarbon shows in shallow wells SZK01-04 in the Jinyang Basin (Li et al., 2014; Zhang et al., 2015; Zhang T. et al., 2017). Core samples revealed extensive black mudstone deposits with gravity flow characteristics and the presence of volcaniclastic deposits, highlighting significant discrepancies in rock types and sedimentary facies compared to previous understandings.

The widespread presence of storm deposits and gravity flow deposits helps explain the occurrence of type III kerogen in the deep-lake fine-grained sediments (Figure 13D). Plant fragments from the deltas, which are the source of type III kerogen, could have been transported by gravity flows triggered by sediment overloading, storm disturbances or earthquakes. Given the common volcanic activity during the Yanshan Orogeny, seismic events could have frequently induced delta failure, transporting plant fragments to deep-water settings. The Beipiao Formation is formed during the Yanshan orogenic event with intensive faulting activity (Sun QS. et al., 2019), which may induce the frequency of earthquakes in the study area. Additionally, hyperpycnal flow could serve as an alternative mechanism, carrying plants and coal fragments into the deep-water basin. The warm and hot climate in the Early Jurassic may also favor the flooding event. From another perspective, the storm wave and gravity flow may also introduce the oxygen into the deep lake basin, reducing the preservation potential of organic matter. However, the relatively high TOC of Beipiao black shale suggests that such sedimentary processes have limited influences on organic matter preservation.

Based on these findings, we propose the following: (1) The Western Liaoning region was a single large lacustrine basin during the depositional period of the Beipiao Formation, rather than consisting of several smaller basins. The uplifts that later divided the Liao Depression were the result of activity along the Nantianmen Fault after the Beipiao Formation was deposited, as supported by several previous studies (Liu and Li, 1997). (2) A widely developed deep lake formed during the deposition of the middle Beipiao Formation, indicating that the development of organic shale has been underestimated, revealing substantial hydrocarbon potential in the study area. (3) Gravity flow, whether caused by delta sediment failure due to sediment overloading, storm disturbances or seismic activity, or by hyperpycnal flow, contributed additional organic material to the black shale of the Beipiao Formation. (4) Clastics from volcanic activity were transported into the deep-water environment by rivers, hyperpycnal flow, or volcanic ash hypopycnal flow, contributing additional sediments. The volcanic processes will be discussed in the following section. Based on these observations and interpretations, we developed a depositional model summarizing the depositional processes from the basin margin to the deep-water basin (Figure 14). The earthquake, flooding induced by heavy raining, storm disturbance and volcanic activity have triggered the sediment failure and density flow that contribute abundant plant fragments (type III kerogen) to the deep-lake basin.

## 7.2 Volcanic process

As previously mentioned, volcanic lava, volcanic breccia, and massive tuff are extensively developed in the study area, indicating that the region has undergone significant volcanic activity. Based on the identification and classification of lithofacies in cores, combined with field lithofacies distribution and sedimentary facies classification, the volcanic processes in the study area can be categorized into three types: volcanic breccia deposits, volcanic hyperpycnal flow deposits, and volcanic ash buoyant flow deposits. Below is an analysis of these volcanic processes and their genesis.

### 7.2.1 Volcanic breccia deposits

In well SZK03, clear evidence of volcanic breccia can be seen, distributed within thick mudstone units. The volcanic breccia fragments are sub-angular, poorly sorted, and matrix-supported, with a fine-grained tuff matrix, indicating deep-water clastic flow deposits influenced by volcanic activity and located relatively far from the volcanic crater. Pyroclasitc flow deposits are high-density clastic flows consisting of volcanic debris ejected during eruptions, which flow along low-lying areas near the volcanic crater under a subaqueous medium, mix with local deposits, and cool and compact to form rock. Volcanic breccia results from fallout of coarse clastic fragments after a volcanic eruption, deposited locally with a short transport distance. Coarse volcanic debris flows can easily incorporate the underlying fine-grained tuff during transport, and due to the influence of water flow, underwater volcanic breccia typically has finer grain sizes and better rounding compared to land-based volcanic debris.

### 7.2.2 Hyperpycnal flow deposits

Broadly speaking, hyperpycnal flows occur when two fluids of similar but slightly different densities mix, resulting in relative movement due to the density difference under suitable environmental conditions. In this study, hyperpycnal flows are primarily composed of volcanic products like fine volcanic dust, which sink into the surface water, creating a density difference between the surface water and the bottom water near the volcanic crater. Under suitable conditions, this leads to the formation of hyperpycnal flow deposits.

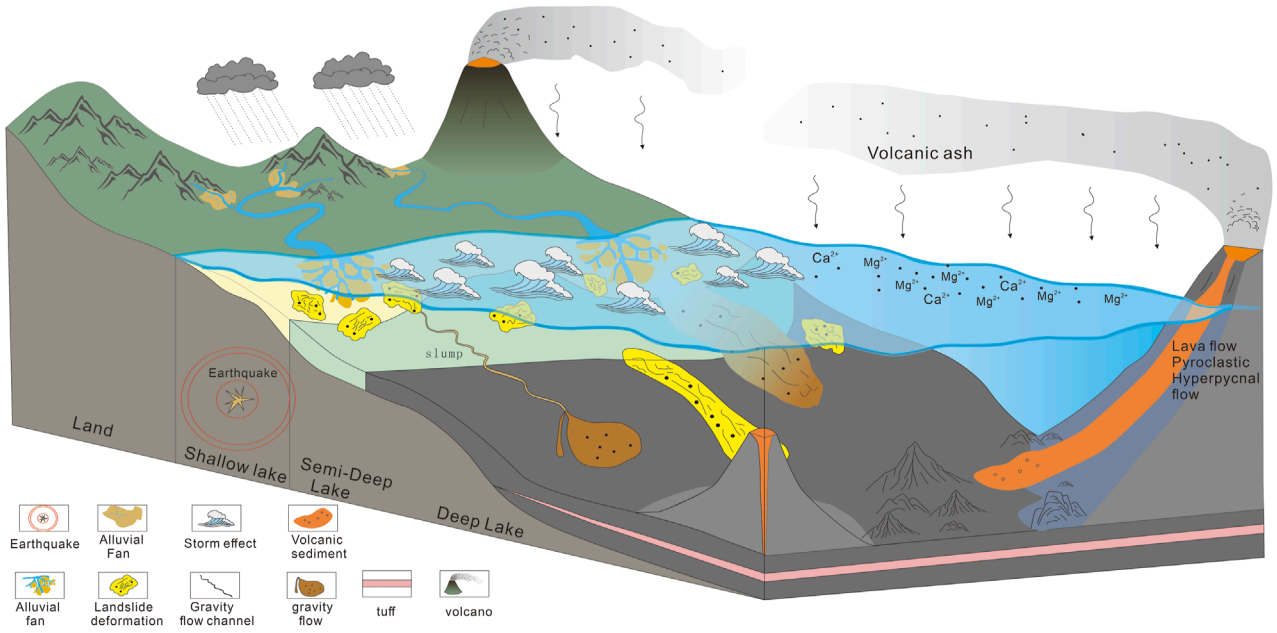


FIGURE 14
Depositional pattern of the Beipiao Formation in the Western Liaoning, Northeast China.

Several types of tuffs are developed in the study area, including massive fine-grained tuff, laminated tuff, massive tuff, and medium to coarse-grained tuff. The medium to coarse-grained tuff was transported along volcanic slopes by hyperpycnal flows and rapidly deposited in the lake basin, forming massive structures with angular volcanic clasts at the base, which are generally poorly sorted and poorly rounded. Medium to coarse-grained volcaniclastic hyperpycnal flows show abrupt contact with the underlying gray-black tuffaceous mudstone. Another portion of medium to coarse volcanic debris was deposited in a semi-consolidated state on volcanic slopes or breaks, and under the influence of volcanic activity, earthquakes, or storms, it lost stability and moved downslope, resulting in slumping deformation. Massive fine-grained tuff traveled longer distances than medium to coarse volcanic debris, reaching further from the volcanic crater, thus having relatively finer grain sizes. The overall color is gray, with a massive structure, lacking other bedding or grading structures. Its genesis may be related to volcanic eruptions involving highly viscous fine volcanic ash that moved along volcanic slopes through hyperpycnal flows and was rapidly deposited.

### 7.2.3 Volcanic ash hypopycnal flow deposits

In a broad sense, hypopycnal flows refer to the movement of two fluids of similar but slightly different densities, with the less dense fluid on top known as a hypopycnal flow. In this study, volcanic ash hypopycnal flow deposits are formed when hot magma comes into contact with cooler lake water, generating large amounts of steam and releasing significant energy, resulting in intense fragmentation. The fine-grained components formed during this fragmentation float upwards due to buoyancy. During this process, the fluid is gradually diluted by the lake water, and its density decreases until it matches that of the surrounding water, at which point the volcanic ash separates from the fluid and slowly settles in suspension. As the energy of the volcanic ash hyperpycnal flow diminishes, hypopycnal flows continue transporting the volcanic ash at the water surface over long distances into the deep lake area, resulting in finer material. In the study area, fine volcanic ash often co-deposits with terrigenous muddy material and carbonate, forming laminated tuffaceous mudstone and tuffaceous carbonate.

The input of terrigenous material into the lake, combined with the effects of hypopycnal volcanic ash flows and the slow suspension deposition of volcanic fine particles, resulted in the development of laminated tuffaceous mudstone and laminated tuffaceous carbonate in the study area. Microscopic examination of laminated tuffaceous mudstone reveals alternating dark muddy laminae and bright tuffaceous laminae. Areas with a higher proportion of dark laminae indicate a volcanic quiescence period, with a lower supply of volcanic glass shards, dominated by terrigenous muddy material. Areas with a higher proportion of bright laminae indicate active volcanic periods with abundant volcanic glass shards. The alternating pattern of bright and dark laminae is the result of alternating deposition of hypopycnal volcanic ash and terrigenous mud in a suspended state in the lake environment, possibly linked to the pulse-like nature of volcanic eruptions.

### 7.2.4 Volcanic process and organic enrichment in shales

Many previous studies found that the toxic effects of volcanic ash eruptions can lead to massive biological extinction. Additionally, volcanic materials coming into contact with lake water during eruptions can cause acidification of the water, resulting in large-scale mortality of organisms due to the unfavorable conditions.

This leads to rapid burial and deposition of abundant hydrocarbon precursors, forming thick sequences of high-quality source rocks, which provide the necessary conditions for hydrocarbon generation in the study area (Wang et al., 2013; Kamo et al., 2003; Schoene et al., 2015).

On the other hand, nutrients transported by volcanic ash may promote biological prosperity (Zhou et al., 1989; Duggen et al., 2007; Langmann et al., 2010; Olgun et al., 2013; Wang et al., 2013; Wu et al., 2018; Qu et al., 2019b; Guo et al., 2021). When volcanic gas particles (containing acids and water-soluble metal salts) adsorbed on the surface of volcanic ash dissolve in water, they release large amounts of nutrients and trace metals, which can increase the primary productivity of seawater, leading to massive reproduction of algae, bacteria, and other organisms (Frogner et al., 2001). The iron content in volcanic ash promotes chlorophyll synthesis and photosynthesis (Coale et al., 1996; Geider, 1999) and enhances nutrient bioavailability (Coale et al., 1996; Takeda, 1998), which facilitates phytoplankton blooms (Yao et al., 2010). Furthermore, the hot climate resulting from volcanic eruptions can create a reducing environment in stagnant, isolated bodies of water. Tuffaceous material supplies ions such as $Ca^{2+}$ and $Mg^{2+}$, increasing the salinity of lake water and creating stratification, which maintains a stable reducing environment at the calm lake bottom, thereby favoring the preservation of organic matter (Qu et al., 2019a).

In this study, we found that the organic rich shale is commonly associated with the massive or fine-grained tuff, tuffaceous siltstone and mudstone (lithofacies 4, five and 6; Table 1 and Figure 4). The black shale shows a relatively high TOC which might be related to the nutrients provided by volcanic activity. We observed widely developed gravity flow, which may introduce oxygen to deepwater and is not favorable to preserve organic matters. However, the volcanic eruptions provide large amounts of clasts into the lake and induce the stratification of the lake, which could help create a reducing environment and favor the preservation of the organic matter. Therefore, we think that the volcanic activity had increased the productivity of the organic matter in the shallow water and help create a reducing environment to preserve the organic matter, which final lead to the high TOC of the black shale in the Jurassic Beipiao Formation.

As a less-explored basin, many aspects of volcanic activity, depositional processes, and the development of organic-rich black shales remain poorly understood. Future research and additional data will be crucial for advancing our knowledge in this area. For instance, petrographic analyses, element analyses mf shales or isotopic studies on kerogen types could help determine the origin of organic matter and clarify the hydrodynamic processes that transport it, particularly in the basin center, where organic matter is most concentrated.

Although more data gained will increase our understanding the organic matter enrichment and fine-grained black shale depositional mechanisms, our current findings are consistent with several studies conducted in the Yanshan orogenic belt region. For example, Zhang et al. (2021) investigated the Cretaceous Jiufotang Formation in the Luanping Basin, located within the Yanshan orogenic belt, and suggested that volcanic activity and a warm climate were the primary factors driving the deposition of thick organic-rich black shales (with an average organic content of 1.39% and Ro values ranging from 0.84% to 1.21%), which exhibit significant hydrocarbon potential in volcanic-rift basins. Similarly, studies in the Cretaceous Jiufotang Formation of the Chaoyang Basin in western Liaoning, adjacent to our study area, indicate that volcanic activity, gravity flow, hydrothermal intrusion, and microbial activity have all played crucial roles in the production and preservation of organic matter (Li et al., 2020; Zhang et al., 2024). Comparable phenomena have also been observed in the Jiufotang Formation of the Fuxin Basin, where sediment supply, hydrothermal intrusion, and gravity flow have shaped both the basin structure and the black shale deposits (Jia et al., 2021). These studies highlight that volcanic activity and gravity flow are common geological processes in volcanic-rift basins of the Northeastern Yanshan orogenic belt, promoting the development of deep-lake, organic-rich black shale deposits and indicating significant, yet often overlooked, hydrocarbon potential.

## 8 Conclusions

This study presents a detailed analysis of the Beipiao Formation in the Beipiao-Jinyang Basin of the western Liaoning province, northeast China, focusing on the lithofacies, sedimentary facies, and the influence of volcanic and depositional processes on hydrocarbon potential. The lithofacies types were identified and classified into 13 categories, including volcanic breccia, tuff, and sedimentary structures indicative of gravity and density flow processes. These lithofacies highlight the significant role that both volcanic and gravity-driven depositional processes played in shaping the basin's stratigraphy.

The basin's evolution transitioned from fan delta to lacustrine environments, with volcanic activity playing a key role in organic matter enrichment. Middle to deep lacustrine deposits, associated with volcanic events, created favorable conditions for preserving organic-rich shales, highlighting the potential for hydrocarbon accumulation.

Geochemical analyses indicate that the organic matter is primarily Type II kerogen, derived from higher plants and aquatic organisms, with moderate to good hydrocarbon potential. The organic matter is at its oil-generation peak in areas with slightly shallower water depths and thinner strata (e.g., well Guan 1). In areas of the basin center (e.g., wells SZK01-04), the organic matter reaches high to over-mature stages, which are more suitable for gas generation.

The interplay between volcanic activity and lacustrine processes led to high-quality source rocks, suggesting significant hydrocarbon potential in the Beipiao Formation, particularly in the deeper lacustrine and volcaniclastic facies. The analysis presented in this work regarding the influence of volcanic activity and gravity flow on organic enrichment, transportation, and preservation can also serve as a valuable reference for investigating other volcanic-lacustrine basins that have developed under comparable geological conditions.

Future exploration should focus on these areas, e.g., areas adjacent to wells SZK01-04 located where deep lake and organic rich shale are developed, to unlock the basin's hydrocarbon resources. Furthermore, this study demonstrates the significant

hydrocarbon potential within this underexplored area, suggesting that similar potential resources may be found in other Jurassic basins formed under comparable tectonic settings in northeast China.

## Data availability statement

The raw data supporting the conclusions of this article will be made available by the authors, without undue reservation.

## Ethics statement

Written informed consent was obtained from the individual(s) for the publication of any potentially identifiable images or data included in this article.

## Author contributions

JW: Writing–original draft, Writing–review and editing. JX: Writing–original draft, Writing–review and editing. ZJ: Conceptualization, Methodology, Resources, Writing–review and editing. TL: Conceptualization, Investigation, Writing–original draft, Writing–review and editing. JM: Conceptualization, Data curation, Writing–review and editing. JZ: Conceptualization, Data curation, Writing–review and editing. SW: Investigation, Writing–review and editing. ZS: Investigation, Methodology, Writing–review and editing. YL: Conceptualization, Investigation, Methodology, Resources, Writing–review and editing. XZ: Investigation, Writing–review and editing.

## Funding

The author(s) declare that financial support was received for the research, authorship, and/or publication of this article. This work is supported by China National Natural Science Foundation of China (No. 41902108). This work is also supported by Hainan Institute of China University of Geosciences, Beijing (No. HNPY-202401) and the Chinese "111" project (B20011).

## Conflict of interest

Author XZ was employed by SINOPEC Northeast Oil & Gas Branch, Exploration and Development Research Institute.

The remaining authors declare that the research was conducted in the absence of any commercial or financial relationships that could be construed as a potential conflict of interest.

## Generative AI statement

The author(s) declare that no Generative AI was used in the creation of this manuscript.

## Publisher's note



## References

Aarnes, I., Planke, S., Trulsvik, M., and Svensen, H. (2015). Contact metamorphism and thermogenic gas generation in the Vøring and Møre basins, offshore Norway, during the Paleocene-Eocene thermal maximum. *J. Geol. Soc.* 172 (5), 588–598. doi:10.1144/jgs2014-098

Aarnes, I., Svensen, H., Connolly, J. A. D., and Podladchikov, Y. Y. (2010). How contact metamorphism can trigger global climate changes: modeling gas generation around igneous sills in sedimentary basins. *Geochimica Cosmochimica Acta* 74 (24), 7179–7195. doi:10.1016/j.gca.2010.09.011

Abrajevitch, A., Andrew, P. R., and Kazuto, K. (2014). Volcanic iron fertilization of primary productivity at kerguelen plateau, southern ocean, through the middle miocene climate transition. *Palaeogeogr. Palaeoclimatol. Palaeoecol.* 410, 1–13. doi:10.1016/j.palaeo.2014.05.028

Chen, S. W., Ding, Q. H., Zheng, Y. J., Li, Y. F., Zhang, J., Wang, J., et al. (2013). New areas and series of strata on the periphery of Songliao Basin: the progress and recognition based on foundational geological survey for oil and gas resources. *Geol. Bull. China* 32 (8), 1147–1158. doi:10.3969/j.issn.1671-2552.2013.08.002

Coale, K. H., Steve, E. F., Gordon, R. M., Johnson, K. S., and Barber, R. T. (1996). Control of community growth and export production by upwelled iron in the equatorial Pacific Ocean. *Nature* 379, 621–624. doi:10.1038/379621a0

Dong, S., Zhang, Y., Li, H., Shi, W., Xue, H., Li, J., et al. (2018). The yanshan orogeny and late mesozoic multi-plate convergence in east asia—commemorating 90th years of the "yanshan Orogeny". *Sci. China Earth Sci.* 61, 1888–1909. doi:10.1007/s11430-017-9297-y

Dou, L. X., Hou, J. G., Song, S. H., Zhang, L., Liu, Y., Sun, S., et al. (2020). Sedimentary characteristics of hyperpycnites in a shallow lacustrine environment: a case study from the lower cretaceous Xiguayuan Formation, Luanping Basin, northeast China. *Geol. J.* 55 (5), 3344–3360. doi:10.1002/gj.3599

Du, X. B., Jia, J. X., Zhao, K., Lu, Y. C., Tan, C., Lu, Y. B., et al. (2022). Development characteristics of deep-time volcanic ash layers and its influence on deposition of organic-rich shale across Ordovician—silurian transition in Yangtze area, south China. *Zhongnan Daxue Xuebao (Ziran Kexue Ban)/Journal Central South Univ. Sci. Technol.* 53 (9), 3509–3521. doi:10.11817/j.issn.1672-7207.2022.09.017

Duggen, S., Croot, P., Schacht, U., and Hoffmann, L. (2007). Subduction zone volcanic ash can fertilize the surface ocean and stimulate phytoplankton growth: evidence from biogeochemical experiments and satellite data. *Geophys. Res. Lett.* 34 (1). doi:10.1029/2006gl027522

Fan, T. G., Xu, X. F., Fan, L., Feng, Y. Q., Liu, W. H., Liu, J. T., et al. (2021). Geological characteristics and exploration prospect of shale oil in permian Lucaogou Formation, Santanghu Basin. *China Pet. Explor.* 26 (4), 125–136. doi:10.3969/j.issn.1672-7703.2021.04.010

Fan, X. J. (2004). *The analysis and evaluation of petroleum geological condition in jinlingsi-yangshan basin*. Liaoning: Liaoning University of Technology.

Felipe, R., Hector, J. V., and Roger, B. (2007). "Hydrocarbon generation, migration, and accumulation related to igneous intrusions: an atypical petroleum system from the Neuquen Basin of Argentina," in *SPE 10th Latin American and caribbean petroleum engineering conference, X LACPEC 07*.

Feng, Z. Z. (2022). Some new thoughts on definitions of terms of sedimentary facies: based on Miall's paper (1985). *J. Palaeogeogr. Chin. Ed.* 24 (2), 183–190. doi:10.7605/gdlxb.2022.02.027

Frogner, P., Gislason, S. R., and Niels, O. (2001). Fertilizing potential of volcanic ash in ocean surface water. *Geology* 29 (6), 487–490. doi:10.1130/0091-7613(2001)029<0487:fpovai>2.0.co;2

Geider, R. J. (1999). Biological oceanography: complex lessons of iron uptake. *Nature* 400 (6747), 815–816. doi:10.1038/23582

Guo, Y., Nishizawa, T., Sakagami, N., Fujimura, R., Kamijo, T., and Ohta, H. (2021). Root bacteriome of a pioneer grass Miscanthus condensatus along restored vegetation on recent Miyake-jima volcanic deposits. *Rhizosphere* 19, 100422. doi:10.1016/j.rhisph.2021.100422

He, B., Fu, Q. P., and Zhang, Y. M. (2006). *Beipiao group hydrocarbon material distribution and organic matter abundance of Jinlingsi—yangshan basin in western part of Liaoning*. Liaoning: Journal of Liaoning Technical University, 24–27.

Jia, J., Wu, Y., Miao, C., Fu, C., Xie, W., Qin, J., et al. (2021). Tectonic controls on the sedimentation and thermal history of supra-detachment basins: a case study of the early cretaceous Fuxin basin, NE China. *Tectonics* 40, e2020TC006535. doi:10.1029/2020TC006535

Jia, L. Q., Wang, L., Wang, G. H., Lei, S., and Wu, X. (2019a). Petrogenesis of the Late Triassic shoshonitic Shadegai pluton from the northern North China Craton: implications for crust-mantle interaction and post-collisional extension. *Geosci. Front.* 10 (2), 595–610. doi:10.1016/j.gsf.2018.08.002

Jia, L. Q., Wang, L., Wang, G. H., Lei, S., and Wu, X. (2019b). Petrogenesis of the Late Triassic shoshonitic Shadegai pluton from the northern North China Craton: implications for crust-mantle interaction and post-collisional extension. *Geosci. Front.* 10 (2), 595–610. doi:10.1016/j.gsf.2018.08.002

Jiang, Z. X., and Chen, D. Z. (2021). *Sedimentology*. Beijing: China Petroleum Publishing House.

Jiang, Z. X., Wang, Y. Z., Wang, L., Kong, X. S., Yang, Y. Q., Zhang, J. G., et al. (2022a). Review on provenance, transport-sedimentation dynamics and multi-source hydrocarbon sweet spots of continental fine-grained sedimentary rocks. *Oil and Gas Geol.* 43 (5), 1039–1048. doi:10.11743/ogg20220503

Jiang, Z. X., Zhang, Y. F., and Yuan, X. D. (2022b). Formation conditions and exploration discoveries of Mesozoic oil and gas in Luanping Basin, Yanshan tectonic belt. *Acta Pet. Sin.* 43 (2), 167–179. doi:10.7623/syxb202202001

Jiao, X., Liu, Y. Q., Zhou, D. W., Li, H., Meng, Z. Y., Zhao, M. R., et al. (2021). Progress on coupling relationship between volcanic and hydrothermal-originated sediments and hydrocarbon generation in lacustrine source rocks. *J. Palaeogeogr. Chin. Ed.* 23 (4), 789–809. doi:10.7605/gdlxb.2021.04.040

Kamo, S. L., Czamanske, G. K., Amelin, Y., Fedorenko, V. A., Davis, D., and Trofimov, V. (2003). Rapid eruption of Siberian flood volcanic rocks and evidence for coincidence with the Permian-Triassic boundary and mass extinction at 251 Ma. *Earth Planet. Sci. Lett.* 214 (1-2), 75–91. doi:10.1016/s0012-821x(03)00347-9

Langmann, B., Zakšek, K., Hort, M., and Duggen, S. (2010). Volcanic ash as fertiliser for the surface ocean. *Atmos. Chem. and Phys.* 10 (8), 3891–3899. doi:10.5194/acp-10-3891-2010

Lee, C. A., Jiang, H. H., Ronay, E., Minisini, D., Stiles, J., and Neal, M. (2018). Volcanic ash as a driver of enhanced organic carbon burial in the Cretaceous. *Sci. Rep.* 8 (1), 4197. doi:10.1038/s41598-018-22576-3

Li, L., Liu, Z. J., Sun, P. C., Li, Y., and George, S. C. (2020). Sedimentary basin evolution, gravity flows, volcanism, and their impacts on the formation of the Lower Cretaceous oil shales in the Chaoyang Basin, northeastern China. *Mar. Petroleum Geol.* 119, 104472. doi:10.1016/j.marpetgeo.2020.104472

Li, Y. F., and Chen, S. W. (2014). New discoveries in oil and gas resources survey at Jiling Temple - yangshan Basin in Liaoxi region. *Geol. Bull. China* 33 (9), 1463–1464. doi:10.3969/j.issn.1671-2552.2014.09.023

Lin, C. F. (2019). *Jurassic tectono-sedimentary evolution history of the western Yanshan fold-thrust belt, North China, and its tectonic implication*. Beijing: China University of Geosciences.

Liu, H. (2019). *Analysis and evaluation of mesozoic intermountain basins groups in western liaoning and its peripheral areas*. Beijing: China University of Geosciences.

Liu, J. J., and Li, Y. H. (1997). Nantianmen Fault in the west liaoning province and its relationship with the development of Beipiao Formation. *Liaoning Geol.* (2), 91–98.

Liu, X. N., Jiang, Z. X., Yuan, X. D., Chen, C., and Wang, C. (2022). Influence of the Cretaceous fine-grained volcanic materials on shale oil/gas, Luanping Basin. *Oil and Gas Geol.* 43 (2), 390–406. doi:10.11743/ogg20220212

Lu, X. Z., Shen, J., Guo, W., and Feng, Q. (2021). Influence of mercury geochemistry and volcanism on the enrichment of organic matter near the Ordovician-Silurian transition in the Middle and Upper Yangtze. *Editor. Comm. Earth Science-Journal China Univ. Geosciences* 46 (7), 2329–2340. doi:10.3799/dqkx.2020.258

Lu, Y. B., Hao, F., Lu, Y. C., Yan, D. T., Xu, S., Shu, Z. G., et al. (2020). Lithofacies and depositional mechanisms of the Wufeng-Longmaxi organic-rich shales in the upper Yangtze area, south China. *AAPG Bull.* 104 (1), 97–129. doi:10.1306/04301918099

Lu, Y. B., Hao, F., Shen, J., Lu, Y. C., Song, H. Y., Wang, Y. C., et al. (2022). High-resolution volcanism-induced oceanic environmental change and its impact on organic matter accumulation in the Late Ordovician Upper Yangtze Sea. *Mar. Petroleum Geol.* 136, 105482. doi:10.1016/j.marpetgeo.2021.105482

Olgun, N., Duggen, S., Andronico, D., Kutterolf, S., Croot, P. L., Giammanco, S., et al. (2013). Possible impacts of volcanic ash emissions of Mount Etna on the primary productivity in the oligotrophic Mediterranean Sea: results from nutrient-release experiments in seawater. *Mar. Chem.* 152, 32–42. doi:10.1016/j.marchem.2013.04.004

Pan, S. X., Liu, H. Q., Zavala, C., Liu, C., Liang, S., Zhang, Q., et al. (2017). Sublacustrine hyperpycnal channel-fan system in a large depression basin: a case study of Nen 1 Member, Cretaceous Nenjiang Formation in the Songliao Basin, NE China. *Petroleum Explor. Dev.* 44 (6), 911–922. doi:10.1016/s1876-3804(17)30103-9

Qiu, Z., Zou, C. N., Li, X. Z., Wang, H. Y., Dong, D. Z., Lu, B., et al. (2018). Discussion on the contribution of graptolite to organic enrichment and reservoir of gas shale: a case study of the Wufeng-Longmaxi Formations in South China. *Nat. Gas. Geosci.* 29 (5), 606–615. doi:10.11764/j.issin.1672-1926.2018.04.005

Qu, C. S., Qiu, L. W., Cao, Y. C., Yang, Y. Q., and Yu, K. H. (2019b). Sedimentary environment and the controlling factors of organic-rich rocks in the Lucaogou Formation of the jimusar sag, Junggar Basin, NW China. *Petroleum Sci.* 16 (4), 763–775. doi:10.1007/s12182-019-0353-3

Qu, C. S., Qiu, L. W., Yang, Y. Q., Yu, K. H., Tang, L., and Wan, M. (2019a). Environmental response of the permian volcanism in Lucaogou Formation in jimsar sag, Junggar Basin, northwest China. *Seismol. Geol.* 41 (3), 789–802. doi:10.3969/j.issn.0253-4967.2019.03.016

Ren, Y. (2012). *The study of yingcheng formation volcanism influence on hydrocarbon source rock in songtiao basin*. Jilin: Jilin University.

Schoene, B., Samperton, K. M., Eddy, M. P., Keller, G., Adatte, T., Bowring, S. A., et al. (2015). U-Pb geochronology of the Deccan Traps and relation to the end-Cretaceous mass extinction. *Science* 347 (6218), 182–184. doi:10.1126/science.aaa0118

Sun, Q. S., Xiao, F., Gao, X. Y., Zong, W., Li, Y., Zhang, J., et al. (2019b). A new discovery of Mesoproterozoic erathem oil and oil-source correlation in the Niuyingzi area of western Liaoning Province, NE China. *Mar. Petroleum Geol.* 110, 606–620. doi:10.1016/j.marpetgeo.2019.07.048

Sun, S. L., Zhang, T., Liu, M., Li, Y. F., Chen, S. W., Zhang, J., et al. (2019a). Sedimentary environment and genesis of source rocks of Beipiao Formation in Jinyang Basin, western liaoning. *J. Northeast Petroleum Univ.* 43 (6), 1–12. doi:10.3969/j.issn.2095-4107.2019.06.001

Sun, S. P., Liu, Y. S., Zhong, R., Bai, Z. D., Li, J. Z., Wei, H. Q., et al. (2001). Classification of pyroclastic rocks and trend of volcanic sedimentology: a review. *Acta Petrologica Mineralogica* 20 (3), 313~317. doi:10.3969/j.issn.1000-6524.2001.03.014

Takeda, S. (1998). Influence of iron availability on nutrient consumption ratio of diatoms in oceanic waters. *Nature* 393 (6687), 774–777. doi:10.1038/31674

Trabucho-Alexandre, J., Hay, P. L. B., and de Boer, P. L. (2012). Phanerozoic environments of black shale deposition and the Wilson Cycle. *Solid earth* 3 (1), 29–42. doi:10.5194/se-3-29-2012

Wang, G. H., Zhang, C. H., Wang, G. S., and Wu, Z. W. (2001). Tectonic framework of western liaoning province and its evolution during mesozoic. *J. Graduate Sch.* (1), 1–7. doi:10.3969/j.issn.1000-8527.2001.01.001

Wang, H. Z. (1993). *A course in Earth history*. Beijing: Geological Publishing House, 295–298.

Wang, J. (2011). *Tectonic evolution of mesozoic volcanic basins in western liaoning and northern hebei*. Beijing: China University of Petroleum.

Wang, S. R., Song, D. F., and He, D. F. (2013). The enrichment effect of organic materials by volcanic ash in sediments of the Santanghu Basin and the evolutionary pattern of tuffaceous source rocks. *Acta Pet. Sin.* (6), 1077–1087. doi:10.7623/syxb201306006

Wu, G., Li, Z. T., and Wang, W. W. (2004). Geochemical characteristics of the Middle Jurassic volcanic rocks from Haifanggou Formation in western Liaoning area and geological significance. *Acta Petrologica Mineralogica* 23 (2), 97–108. doi:10.3969/j.issn.1000-6524.2004.02.001

Wu, L. Y., Lu, Y. C., Jiang, S., Liu, X., and He, G. (2018). Effects of volcanic activities in ordovician wufeng–silurian longmaxi period on organic-rich shale in the upper Yangtze area, south China. *Petroleum Explor. Dev.* 45 (5), 862–872. doi:10.1016/s1876-3804(18)30089-2

Yan, Y., Lin, G., and Li, Z. A. (2002). Characteristics of the jurassic filling sequence and the indication of tectonic evolution of Beipiao Basin, western liaoning. *J. Stratigr.* (2), 151–155. doi:10.3969/j.issn.0253-4959.2002.02.014

Yan, Y., Lin, G., Li, Z. A., He, S. J., and Xv, Z. Y. (2003). Detrital composition of mesozoic sandstone and its implication for provenance and tectonic evolution of Beipiao (Jin-Yang) basin, western liaoning province. *Acta Sedimentol. Sin.* (3), 441–447. doi:10.14027/j.cnki.cjxb.2003.012

Yao, B., Xi, B. D., Hu, C. M., Ding, J. T., Zhang, J. T., Xv, Q. G., et al. (2010). A review of iron limitation on the growth and competition of phytoplankton. *Ecol. Environ. Sci.* (2), 459–465. doi:10.3969/j.issn.1674-5906.2010.02.039

Yuan, W., Liu, G. D., Xu, L. M., and Niu, X. B. (2019). Main controlling factors for organic matter enrichment in Chang 7 member of the Yanchang Formation, Ordos Basin. *Oil Gas Geol.* 40 (2), 326–334. doi:10.11743/ogg20190211

Yuan, X. D., Jiang, Z. X., Zhang, Y. F., and Jiang, H. F. (2020). Characteristics of the Cretaceous continental shale oil reservoirs in Luanping Basin. *Acta Pet. Sin.* 41, 1197–1208. doi:10.7623/syxb202010004

Zavala, C., and Pan, S. X. (2018). Hyperpycnal flows and hyperpycnites: origin and distinctive characteristics. *Lithol. Reserv.* 30 (1), 1–18. doi:10.3969/j.issn.1673-8926.2018.01.001

Zhang, J. Z., Jiang, Z. X., Xu, J., Wei, S. Y., Song, L. Z., Liu, T., et al. (2024) *Volcanic sedimentation of cretaceous Jiufotang Formation in the Chaoyang Basin and its impact on organic matter enrichment*, 3, 284–297.

Zhang, K., Li, Y. F., Tang, Y. J., Gao, X. Y., Sun, S., Zhou, T. S., et al. (2015). Characteristics of biomarker compounds in oil sands of the Beipiao Formation, liaoxi Jinyang Basin — a case study of well SZK02. *Geol. Rev.* 61 (S1), 198–199.

Zhang, L. S., Xie, M. Z., Zhang, S. S., Zhang, X. S., Shang, H. T., Li, X. H., et al. (2016). Rediscussion on geologic age and regional correlation about Beipiao Formation in western liaoning. *Geol. Rev.* 62 (6), 1392–1402. doi:10.16509/j.georeview.2016.06.003

Zhang, R., Jiang, T., Tian, Y., Xie, S. C., Zhou, L., Li, Q., et al. (2017a). Volcanic ash stimulates growth of marine autotrophic and heterotrophic microorganisms. *Geology* 45 (8), 679–682. doi:10.1130/G38833.1

Zhang, T., Li, Y. F., Sun, S. L., Gao, X. Y., Zhou, T. S., Sun, P., et al. (2017b). Saturated hydrocarbon geochemical characteristics of the oil sand from YD1 well in Jinyang Basin and its significance for oil and gas exploration. *Geol. Bull. China* 36 (4), 582–590. doi:10.3969/j.issn.1671-2552.2017.04.012

Zhang, Y. F., Yuan, X. D., Wang, M., Ge, P., Huo, Y., Xu, J., et al. (2021). Discovery of lacustrine shale deposits in the Yanshan Orogenic Belt, China: implications for hydrocarbon exploration. *Geosci. Front.* 12 (6), 332–359. doi:10.1016/j.gsf.2021.101256

Zhen, Z., Li, Y. F., Gao, X. Y., Sun, S. L., and Zhou, T. S. (2016). Characteristics of sedimentary facies and organic matter of lower jurassic Beipiao Formation of well SZK01 in Jinyang Basin. *Glob. Geol.* (1), 207–215. doi:10.3969/j.issn.1004-5589.2016.01.021

Zhou, L. D., and Zhao, M. P. (1999). Study on evolution history of the fault zone on the west edge of Jinlingsi-Yangshan Basin in West Liaoning. *Liaoning Geol.* (4), 11–16.

Zhou, Z. Y., Sheng, G. Y., and Min, Y. S. (1989). A primary study of tuffaceous source rock by organic geochemistry. *Acta Sedimentol. Sin.* 7 (3), 3–9.

Zou, C. N., Guo, Q. L., Yang, Z., Wu, S., Chen, N., Lin, S., et al. (2019). Resource potential and core area prediction of lacustrine tight oil: the Triassic Yanchang Formation in Ordos Basin, China. *AAPG Bull.* 103 (6), 1493–1523. doi:10.1306/11211816511